Cullin E3 Ligase Activity Is Required for Myoblast Differentiation

Jordan Blondelle [1], **Paige Shapiro** [1], **Andrea A. Domenighetti** [2,3] and **Stephan Lange** [1]

1 - *Division of Cardiology,* University of California San Diego, La Jolla, CA-92093 USA
2 - *Rehabilitation Institute of Chicago,* Chicago, IL-60611 USA
3 - *Department of Physical Medicine and Rehabilitation,* Northwestern University, Chicago, IL-60611, USA

Correspondence to Stephan Lange: UC San Diego, School of Medicine, 9500 Gilman Drive, BRF2 #1243, La Jolla, CA 92093, USA. slange@ucsd.edu
http://dx.doi.org/10.1016/j.jmb.2017.02.012
Edited by M Yaniv

Abstract

The role of cullin E3-ubiquitin ligases for muscle homeostasis is best known during muscle atrophy, as the cullin-1 substrate adaptor atrogin-1 is among the most well-characterized muscle atrogins. We investigated whether cullin activity was also crucial during terminal myoblast differentiation and aggregation of acetylcholine receptors for the establishment of neuromuscular junctions *in vitro*.

The activity of cullin E3-ligases is modulated through post-translational modification with the small ubiquitin-like modifier nedd8. Using either the Nae1 inhibitor MLN4924 (Pevonedistat) or siRNA against nedd8 in early or late stages of differentiation on C2C12 myoblasts, and primary satellite cells from mouse and human, we show that cullin E3-ligase activity is necessary for each step of the muscle cell differentiation program *in vitro*. We further investigate known transcriptional repressors for terminal muscle differentiation, namely ZBTB38, Bhlhe41, and Id1. Due to their identified roles for terminal muscle differentiation, we hypothesize that the accumulation of these potential cullin E3-ligase substrates may be partially responsible for the observed phenotype.

MLN4924 is currently undergoing clinical trials in cancer patients, and our experiments highlight concerns on the homeostasis and regenerative capacity of muscles in these patients who often experience cachexia.

Introduction

Skeletal muscle mass represents up to 40% of the young adult body weight. Its maintenance is regulated by the equilibrium between muscle growth or physiological hypertrophy and muscle atrophy, which is reflected on the cellular level by the balance between protein synthesis and degradation. While hypertrophy relies mainly on the activation of the Phosphatidylinositol 3-kinase and mammalian target of rapamycin (PI3K–mTOR) signaling pathway, immobilization, denervation, aging, or diseases such as cancer may induce muscle atrophy [1]. In muscle cells, the autophagy–lysosome and the ubiquitin–proteasome systems (UPSs) are the main protein degradation mechanisms [2,3]. In particular, the UPS is responsible for the degradation of the majority of cytoplasmic proteins [4].

The UPS requires the tagging of substrates by ubiquitin via an enzymatic cascade [4,5]. First, the E1-ubiquitin activating enzyme covalently attaches to ubiquitin through an ATP-driven step. Once activated, ubiquitin is transferred to E2-ubiquitin conjugating enzymes. The last step requires the concerted action of an E2-enzyme and an E3-ubiquitin ligase, which transfer the ubiquitin from the E2-enzyme onto the substrate. Once poly-ubiquitylated, the substrate is targeted to the proteasome for degradation.

Cullin-RING (really interesting new gene) ligases (CRLs) represent the largest family of E3-ubiquitin ligases in mammalian cells [6,7]. In order to form CRL complexes, each cullin, which forms the backbone of the E3-ligase complex, interacts modularly with RING (really interesting new gene) domain proteins Rbx1 or Rbx2 that are in turn bound to E2-enzymes. Each member of the cullin protein family binds also to a

specific subset of adaptor proteins, thereby achieving specificity for a range of cellular substrates. The activity of CRL is regulated by the post-translational modification of the cullin protein with the small ubiquitin-like protein nedd8 [6–8]. The essential role of CRL for adult muscle homeostasis has been
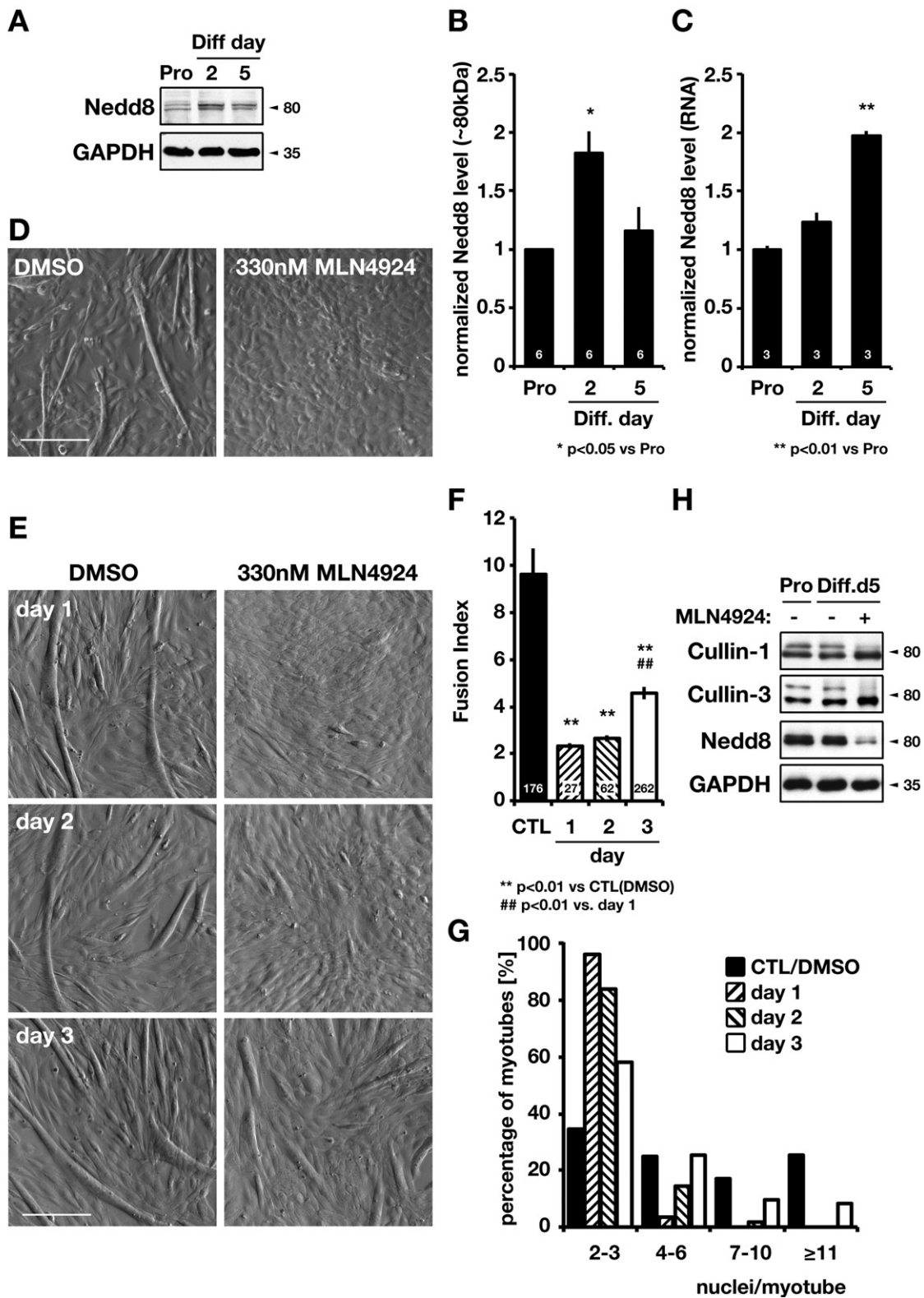

Fig. 1 (*legend on next page*)

unraveled by the discovery that nedd8 is almost exclusively expressed in muscles [9], and the discovery of the requirement of cullin-1 and its substrate adaptor atrogin-1 (MAFbx, Fbxo32), to mediate muscle atrophy [10]. However, while largely uncharacterized, there is an emerging role for other substrate adaptors for cullin-1 and CRL complexes that are formed by other cullin proteins, like cullin-3, for myogenesis and skeletal muscle development [11].

In the last 20 years, the role of CRLs has been mainly investigated in the context of cancers, revealing a plethora of functions relevant for carcinogenesis [12,13]. So far, many of the identified CRL substrates play a role in cell cycle progression [14], such as Cyclin E [15,16] that is a gatekeeper of the passage from the G1 phase to the S phase. Therefore, CRL recently became an attractive potential anticancer target [17], and the discovery of inhibitors of cullin neddylation, such as MLN4924, opened new therapeutic avenues [14]. MLN4924 is currently undergoing clinical trials for various cancer types [18,19].

Cancer patients may develop cachexia, a deleterious wasting syndrome that is associated with muscle atrophy and has an impact on the well-being of patients and on the response to the treatment. Indeed, cachexia is a devastating and often irreversible syndrome observed in up to 80% of cancer patients [20]. Most importantly, cachexia has been shown to be responsible for the death of 20% of all cancer patients [21,22]. In mice, defects in skeletal muscle regeneration and satellite cell differentiation due to a deregulation of Pax7 expression have been demonstrated to contribute to cancer cachexia [23]. Indeed, the efficiency of muscle mass and its maintenance in cancer patients has been used as an independent predictor of mortality in some cancers [24,25] and should be closely monitored.

To date, no data are available regarding the effect of a loss of CRL activity on muscle cell differentiation and the effect of MLN4924 on muscle cells. Given the emerging role of CRL substrate adaptors in muscle development and disease [11], we decided to address the function of CRL in myogenesis and myotube formation by using MLN4924 and siRNA experiments.

Our data revealed, for the first time, that CRL activity is required for myoblast differentiation and for the commitment of the skeletal muscle stem cells into the myogenic differentiation program. Our data highlight that MLN4924, a CRL activity inhibitor used currently as a potential cancer therapy, has potentially negative side effects on muscle cell differentiation through, in part, the regulation of myogenin expression. Given the systemic delivery of MLN4924 in cancer patients during clinical trials [18,19], our results suggest the necessity to closely monitor skeletal muscle mass and muscle regeneration in treated patients.

Results

CRL inhibition prevents myotube formation

Cullin activity is known to be important during muscle atrophy, as the cullin-1 substrate adaptor atrogin-1 (MAFbx, Fbxo32) is among the best-characterized muscle atrogins. We set out to investigate whether cullin activity is also changed during muscle differentiation and whether there is a requirement for cullin-mediated protein degradation during myotube formation. Levels of nedd8-modified proteins at approximately 80 kDa, which can be attributed to neddylated versions of cullin-1, cullin-2, cullin-3, cullin-4A, or cullin-5, increased significantly over the first 2 days in differentiation to decrease back to levels found during proliferation (Fig. 1A and B). Intriguingly, this change on the protein level was not mirrored on the RNA level, where total nedd8 mRNA increased more than twofold over the same period (Fig. 1C). The observed increase in neddylation is indicative of changes to cullin activity. We further used the nedd8 activating enzyme E1 subunit 1 (NAE1) inhibitor MLN4924 [26] that interferes with the activation of all

Fig. 1. Cullin E3-ligase activity is required for myotube formation in C2C12 cells. (A) Analysis of proteins modified by nedd8 in C2C12 cells during proliferation (Pro) or during differentiation at day 2 and 5. GAPDH is shown to demonstrate equal loading of the samples. (B) Quantification of GAPDH-normalized nedd8 modified protein levels around 80 kDa [from (A)]. (C) Quantification of nedd8 mRNA levels normalized against cyclophilin B. (B–C) Sample size and *p*-values are shown in the figure. (D) Representative brightfield images of C2C12 after 5 days in differentiation medium. Cells have been treated with vehicle control (DMSO) or 330 nM NAE1 inhibitor MLN4924 from the onset of differentiation. Scale bar represents 40 µm. (E) Representative brightfield images of C2C12 after 5 days in differentiation medium. Cells have been treated with vehicle control (DMSO) or 330 nM NAE1 inhibitor MLN4924 1, 2, or 3 days after the start of differentiation. Scale bar represents 40 µm. (F) Quantification of C2C12 fusion index for C2C12 cells exposed after 1, 2, or 3 days of differentiation starts with 330 nM MLN4924 or vehicle control (DMSO). Sample size and *p*-values are indicated in the figure. (G) Percentage of counted myotubes with 2–3, 4–6, 7–10, or more than 11 nuclei per myotube, from C2C12 cultures exposed to 330 nM MLN4924 after 1, 2, or 3 days of differentiation or vehicle control (DMSO). (H) Immunoblot analyses of cullin-1, cullin-3, and nedd8 expression levels of C2C12 cells in proliferation (Pro) or after 5 days in differentiation (Diff) medium with 300 nM MLN4924 (+) or vehicle control (DMSO, –). GAPDH was used as loading control.
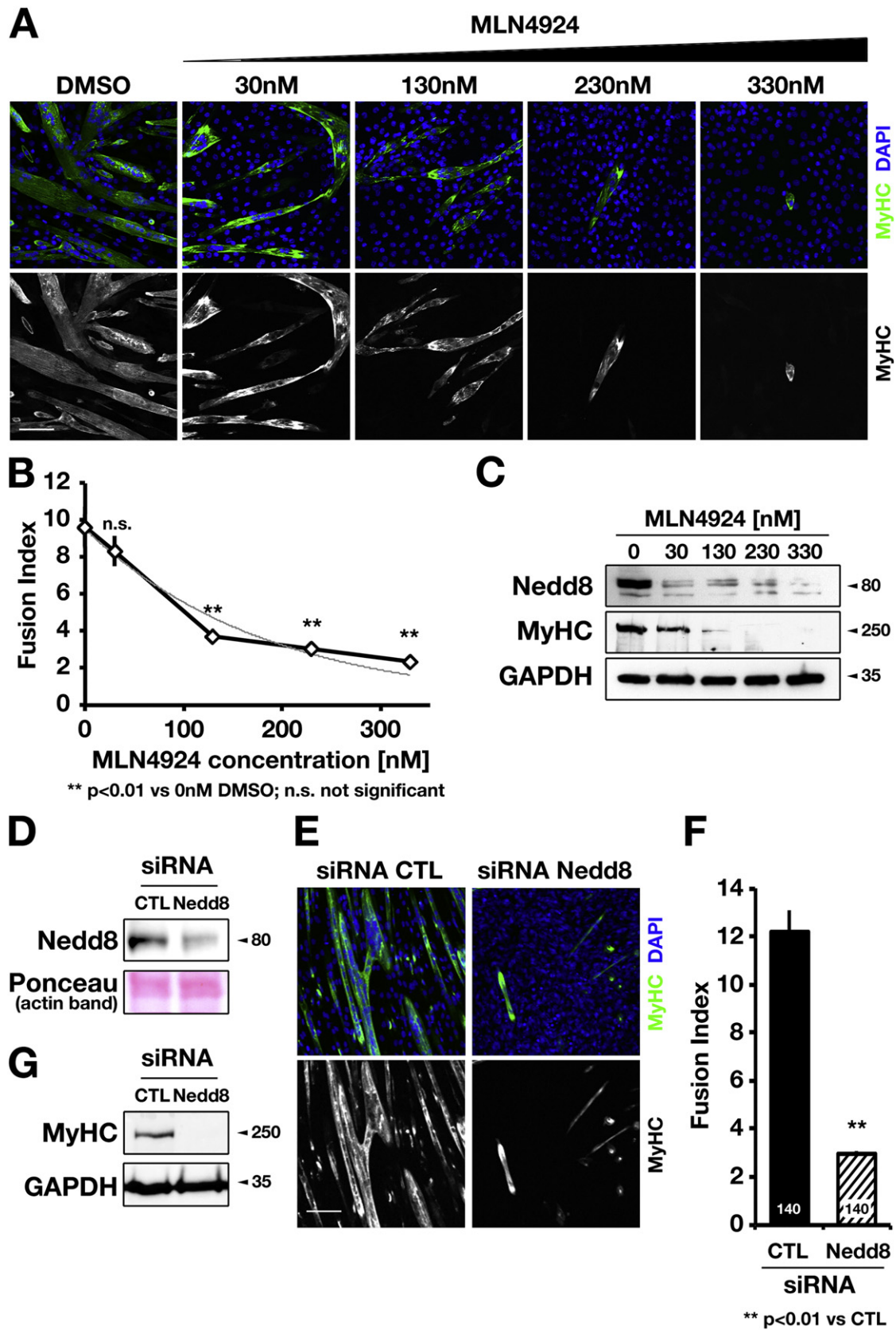
Fig. 2 (legend on next page)

cullin E3-ligases to investigate whether cullin-mediated protein degradation is required for muscle differentiation. Confluent cultures of C2C12 myoblasts were incubated in the presence of 330 nM MLN4924 supplemented to the differentiation medium and allowed to differentiate for 5 days. While the vehicle-treated control cells formed long, multinucleated myotubes, C2C12 cells treated with the inhibitor failed to form myotubes (Fig. 1D). In order to investigate the time point at which cullin activity is critical during myotube formation, we investigated the levels of nedd8-modified proteins over the course of muscle cell differentiation and set up a timed inhibitor treatment experiment. This experiment also tests whether the identified peak for the neddylation of cullin proteins over the first couple of days is important for the differentiation of myoblasts into myotubes. Differentiating C2C12 cultures were treated with MLN4924 1, 2, or 3 days after change into differentiation medium and were cultured for a total of 5 days. Differentiating cells showed a lack of myotube formation upon inhibitor treatment 1 or 2 days after differentiation. However, some myotubes were found when the inhibitor was added 3 days after the start of differentiation (Fig. 1E), as also observed when we measured the fusion index (i.e., number of nuclei per myotube; Fig. 1F). Accordingly, the distribution of nuclei per myotube revealed a strong accumulation of small myotubes containing 2–3 nuclei and a severe decrease in the number of large myotubes containing >7 nuclei after 5 days of differentiation (Fig. 1G). These data indicate that cullin E3-ubiquitin ligase activity is crucial at the onset of the myotube formation at around 1–2 days of differentiation, with a weaker effect at later stages. Cullin protein levels (overall band intensity) and activity (as measured by the super-shifted "neddylated" cullin) return to levels observed in proliferative C2C12 cells 5 days after the start of differentiation for cullin-1 and cullin-3 (Fig. 1H). Treatment with MLN4924 shows decreased or absent cullin activity, congruent with largely reduced nedd8 levels, validating the efficiency of the inhibitor on C2C12 cells (Fig. 1H).

Next, we investigated the dose–response for the effect of cullin inhibition on myotube formation. We treated differentiating C2C12 cells with 30 nM, 130 nM, 230 nM, or 330 nM MLN4924 or with vehicle control. Microscopic brightfield and immunofluorescence images of C2C12 cells 5 days after the start of differentiation indicated that as little as 130 nM MLN4924 was sufficient to significantly reduce the fusion index to about 40% of control levels, with higher doses showing a more severe inhibition of myotube formation (Fig. 2A and B and Supplementary Fig. S1A). Immunoblot analysis of C2C12 cells differentiated with increasing amounts of MLN4924 also show gradual loss of 80-kDa nedd8-modified proteins and sarcomeric myosin heavy chain (MyHC) expression (Fig. 2C), in agreement with a decrease in fusion index (Fig. 2B).

To verify that the inhibition of cullin activity by MLN4924 is specific and works through a deficiency in neddylation, we used small interfering RNA (siRNA). Proliferating C2C12 were transfected with either siRNA directed against nedd8 or a scrambled control and were allowed to differentiate for 5 days. Specific knockdown of nedd8 that results in significantly decreased cullin neddylation at approximately 80 kDa was verified by immunoblots (Fig. 2D and Supplementary Fig. S1B). Inhibition of cullin activity by nedd8 siRNA also led to a reduction in total ubiquitylation, as observed in immunoblot assays (Supplementary Fig. S1C and D). Immunofluorescence analysis of differentiated C2C12 myotubes transfected with siRNA against nedd8 fails to form myotubes (Fig. 2E and Supplementary Fig. S1E), similar to MLN4924-treated cells (Fig. 2A; 330 nM MLN4924). The failure to form multinucleated myotubes in nedd8 siRNA-transfected C2C12 is also reflected in the low fusion index measured for these cells compared to controls (Fig. 2F). Analysis of MyHC expression (Fig. 2G) further validated that C2C12 transfected with siRNA against nedd8 fail to differentiate, similar to MLN4924-treated cells (Fig. 2C).

These data indicate that cullin activity is crucial for the formation of multinucleated myotubes and the expression of key muscle-specific genes, like sarcomeric MyHCs, during terminal muscle differentiation. The action of MLN4924 is specific and inhibits muscle formation in a dose-dependent way.
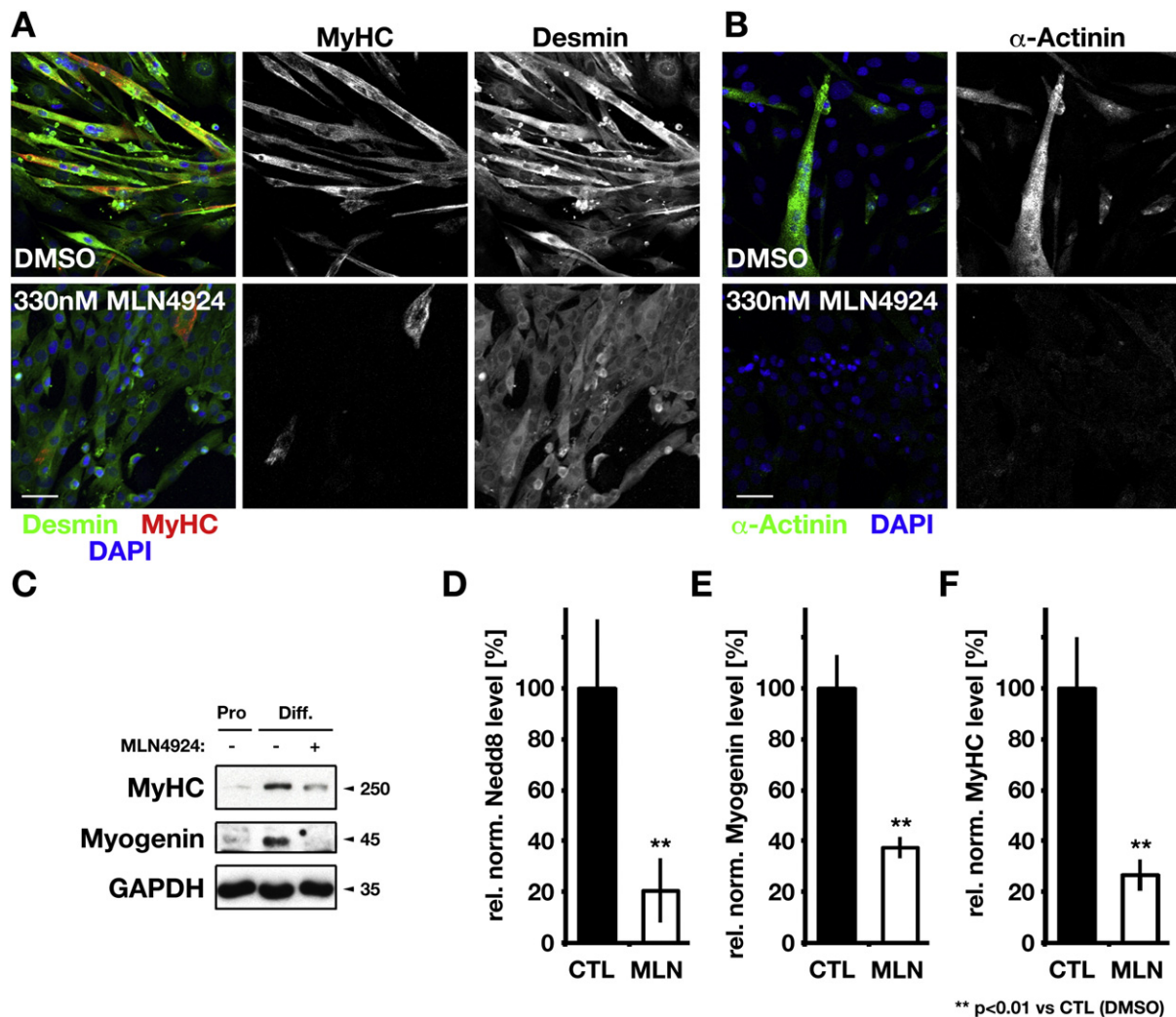
Fig. 2. MLN4924 dose–response curve and nedd8 siRNA. (A) Immunofluorescence analysis of C2C12 cells differentiated for 5 days in the presence of 30 nM, 130 nM, 230 nM, or 330 nM MLN4924 or vehicle control (DMSO). Cells were stained with an antibody against pan-sarcomeric myosin heavy chain (MyHC). DAPI was used as counterstain. Scale bar represents 100 μm. (B) Quantification of fusion index in response to increasing MLN4924 concentrations. Shown are average fusion indexes, standard errors, and *p*-values (indicated in figure). Gray line indicates fitted curve to determine IC$_{50}$ value. (C) Immunoblot analysis of nedd8 and pan-sarcomeric MyHC protein levels in total protein samples of C2C12 cells differentiated for 5 days in the presence of 30 nM, 130 nM, 230 nM, or 330 nM MLN4924 or vehicle control (0 nM MLN4924; DMSO). GAPDH was used as loading control. (D) Immunoblot analysis of nedd8 in C2C12 after 3 days of differentiation. (E and F) Immunofluorescence analysis (E) and fusion index (F) of differentiated C2C12 cells transfected with siRNA against nedd8 or scrambled control (CTL). Cells were differentiated for 5 days and stained with an antibody against pan-sarcomeric MyHC. DAPI was used as counterstain. Scale bar represents 100 μm. Standard errors and *p*-values are indicated in the figure. (G) Immunoblot analysis of pan-sarcomeric MyHC in differentiated C2C12 after 5 days. Ponceau (D) or GAPDH (G) was used as loading controls.

Cullin inhibition prevents entry into the terminal myogenic differentiation program

Because we observed a complete loss of sarcomeric MyHC expression (Fig. 2), we wondered whether nedd8 inhibition interferes globally with the activation of critical muscle genes and entry into the terminal muscle differentiation program. We tested the expression of muscle proteins critical for myofilament formation, like sarcomeric alpha-actinin, using immunofluorescence and immunoblot assays. While MyHC and alpha-actinin expression was upregulated in differentiating control cells, MLN4924-treated cells largely failed to express these muscle proteins crucial for myofibrillogenesis (Fig. 3A and B). Similarly, desmin levels in nedd8 inhibitor-treated cells remain comparable to those found in undifferentiated proliferating myoblasts (Fig. 3A).

Muscle gene expression is regulated by several myogenic transcription factors, including myogenin. We tested myogenin protein levels in inhibitor-treated and vehicle-treated control cells and compared them to

Fig. 3. MLN4924 inhibits entry into the terminal myogenic differentiation program. (A and B) Immunofluorescence analysis of C2C12 cells differentiated for 5 days in the presence or absence of 330 nM MLN4924 stained with antibodies against sarcomeric myosin heavy chain (MyHC) and desmin (A) or alpha-actinin (B). DAPI was used as counterstain in (A and B). Scale bar represents 50 µm. (C) Immunoblot analysis of pan-sarcomeric MyHC and myogenin expression in whole cell lysates of C2C12 cells either in proliferation (Pro) or after 5 days in differentiation (Diff) medium with 300 nM MLN4924 (+) or vehicle control (DMSO, −). GAPDH was used as loading control. (D–F) Relative normalized protein levels of nedd8 protein levels (D; 80-kDa band), myogenin (E), and pan-sarcomeric MyHC (F) in MLN4924 (MLN)-treated C2C12 cells 5 days after differentiation compared to controls (CTL). Three independent samples were run per group; *p*-values are indicated in the figure.

proliferating myoblasts. Intriguingly, myogenin protein levels in MLN4924-treated C2C12 cells remained low, comparable to proliferating myoblast cultures (Fig. 3C). This result indicates that cullin activity is required to enter into the myogenic differentiation program. C2C12 cells treated with MLN4924 show low neddylation levels of cullin proteins (Fig. 3D), fail to enter into the myogenic differentiation program, display a 60% reduction in myogenin protein levels (Fig. 3E), and hence exhibit low expression levels of muscle proteins required for myofibrillogenesis, like sarcomeric MyHC (Fig. 3C and F).

In summary, these data indicate a crucial role for cullin E3-ubiquitin ligase activity in the entry into the terminal myogenic differentiation program, as crucial muscle transcription factors, like myogenin, are not induced upon myoblast differentiation. Consequently, inhibitor-treated cells fail to upregulate muscle-specific proteins, like MyHC or alpha-actinin.

Mouse and human satellite cells treated with MLN4924 fail to differentiate

C2C12 cells were originally isolated from dystrophic mouse muscle [27] but have since been widely used as a standard model for muscle cell differentiation and myofibrillogenesis [28–31]. We wondered whether the findings from this cell line would be reproducible with primary cultures of isolated mouse and human muscle stem cells (satellite cells).

To test this, we freshly isolated muscle stem cells from mouse hind limbs and differentiated them in the presence or absence of MLN4924. Similar to differentiating C2C12 cells, muscle stem cells did not form myotubes in the presence of MLN4924 (Fig. 4A) and failed to enter into the terminal myogenic differentiation program, as MyHC expression was found to be reduced, compared to vehicle-treated controls (Fig. 4B). In resemblance to inhibitor-treated C2C12 cells, the reduction in MyHC parallels the inhibitory effect on cullin activity, as seen in a loss of the neddylated form of cullin-1 (Fig. 4B, upper panel). In addition, the effect of MLN4924 on muscle cell differentiation is also readily observed in human muscle stem-cell-derived myoblasts, which failed to differentiate into myotubes after 3 days in the presence of 330 nM MLN4924, as demonstrated by the lack of multinucleated myotubes expressing MyHC and myogenin (Fig. 4C and D).

Cullin inhibition interferes with acetylcholine receptor (AChR) clustering

We demonstrated that cullin E3-ubiquitin ligase activity is crucial for entry into the terminal myogenic differentiation program and myotube formation. Another important step during skeletal muscle differentiation is the formation of neuromuscular junctions (NMJs).

During NMJ formation, AchRs are densely packed into clusters. This step is initiated by the expression of agrin [32]. *In vitro*, the clustering of AchR can be induced by treating myotubes with neural agrin. We tested if cullin activity is also required for this step in the skeletal muscle differentiation program, by treating differentiated myotubes at day 5 with agrin overnight in the presence or absence of MLN4924. While vehicle-treated control C2C12 myotubes demonstrated AChR clustering upon agrin stimulation, inhibitor-treated control cells showed reduced cluster formation (Fig. 5A). To see whether this effect is statistically significant, we measured several parameters, including myotube length (Fig. 5B), the number of nuclei per myotube (Fig. 5C), the number of AChR clusters per myotube (Fig. 5D), the number of AChR clusters/mm^2 (Fig. 5E), and the AChR cluster length/mm^2 (Fig. 5F). While MLN4924 treatment of differentiated myotubes does not alter myotube length, the number of nuclei per myotube or the number of AChR clusters per myotube, the cluster density (cluster/mm^2), and length (cluster length/mm^2) were slightly but significantly reduced. These data point toward another potential function for cullin activity, in the formation of the neuromuscular junction.

The effects of cullin inhibition on terminal muscle differentiation are reversible

MLN4924 is currently undergoing clinical trials as a potential approach for the treatment of various cancers, including acute myelogenous leukemia [14,33–35]. Drug escalation studies [34] and other clinical trials[†] administer the drug typically either on an intermittent protocol (e.g., on days 1, 4, 8, and 11 of a 2-week protocol) or continuously for up to 5 consecutive days. Analysis of molecular data from mice indicates that MLN4924 disrupts cullin-mediated protein turnover in tumor cells, leading to apoptosis caused by a deregulation of S-phase DNA synthesis [14]. Our data revealed the requirement of cullin activity for myoblast differentiation and led us to question whether the effect of MLN4924 on C2C12 myotube development and terminal differentiation is permanent or reversible.

C2C12 cells undergoing differentiation were treated for 5 days with 330 nM MLN4924 and were subsequently allowed to recover for 5 days in differentiation medium. Cells that were undergoing this treatment were able to differentiate into myotubes (Fig. 6A). These cells also upregulated MyHC and desmin, indicating successful entry into the terminal myogenic differentiation program. When we investigated the fusion index, recovered cells were more comparable to C2C12 cells that were differentiated for 5 days than to C2C12 that were 10 days in the differentiation medium (Fig. 6B). These data suggest that MLN4924 temporarily interrupts myotube formation and muscle cell differentiation but that the effects of the drug are
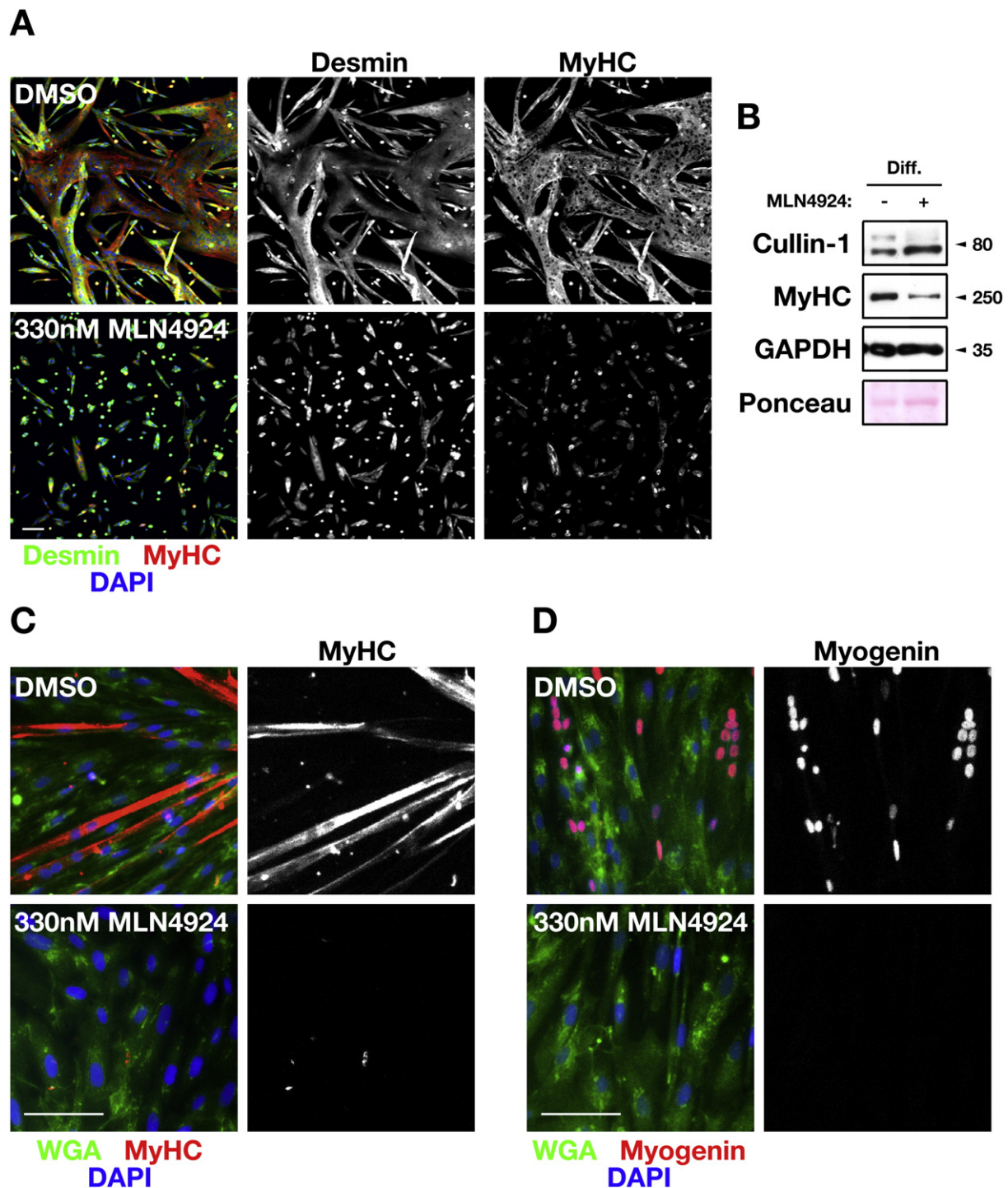
Fig. 4. Cullin E3-ligase activity is required for myotube formation of mouse and human muscle stem cells. (A) Immunofluorescence analysis of primary cultures of mouse muscle stem cells after 5 days of differentiation. Cells were differentiated in the presence of 330 nM MLN4924 or vehicle control (DMSO) and stained with antibodies against desmin and pan-sarcomeric myosin heavy chain (MyHC). DAPI was used as counterstain. Scale bar represents 100 µm. (B) Immunoblot analysis of cullin-1 and pan-sarcomeric MyHC protein levels in total lysates of differentiated primary mouse muscle stem cell cultures treated with 330 nM MLN4924 (+) or vehicle control (DMSO, –). GAPDH and ponceau-stained actin band were used as loading controls. C and D) Immunofluorescence analysis of human muscle stem cells after 5 days of differentiation in the presence of 330 nM MLN4924 or vehicle control (DMSO). Cells were stained with antibodies against slow MyHC (C) or myogenin (D). DAPI and fluorescently labeled wheat germ agglutinin (WGA) were used as counterstains. Scale bar represents 100 µm.
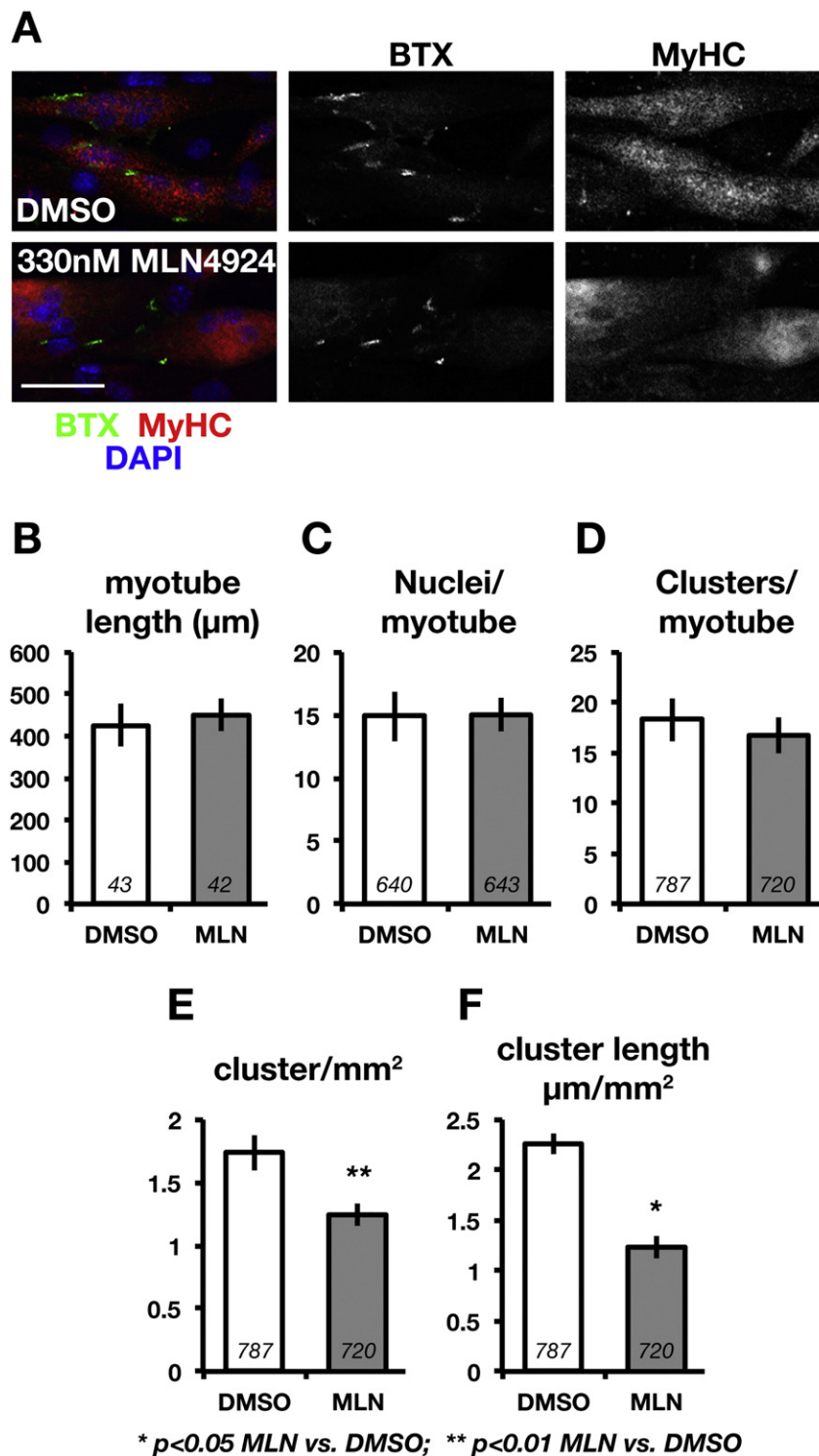
Fig. 5. Effect of cullin E3-ligase inhibition on agrin-induced AChR clustering in C2C12 cells. (A) Immunofluorescence analysis of agrin-treated C2C12 cells 5 days after differentiation in the presence of 330 nM MLN4924 or vehicle control (DMSO). Cells were stained with antibodies against pan-sarcomeric myosin heavy chain (MyHC) and fluorescently labeled alpha-bungarotoxin (BTX) to visualize AChRs. DAPI was used as counterstain. Scale bar represents 50 μm. (B–F) Quantitative analysis of myotube length (B), fusion index (C; nuclei/myotube), number of AChR clusters per myotube (D), AChR cluster number per mm^2 (E), and cluster length per mm^2 (F). Shown are averages and standard errors. Sample size and p-values are indicated in the figure.
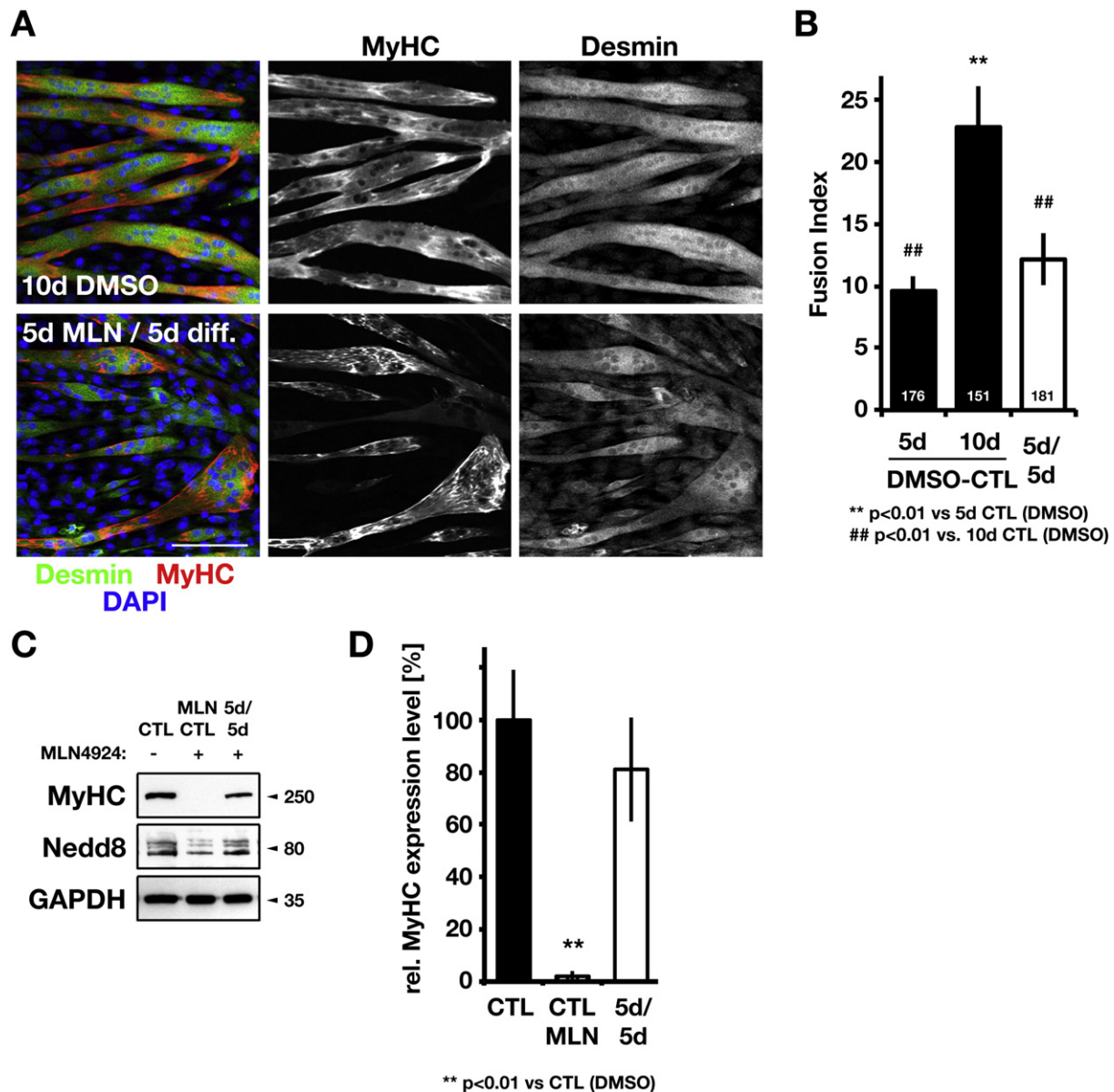
Fig. 6. Effect of cullin E3-ligase inhibition on terminal muscle differentiation is reversible. (A) Immunofluorescence analysis of C2C12 cells after 10 days of differentiation in vehicle (10d DMSO)-supplemented differentiation medium, compared to cells cultured for 5 days in differentiation medium supplemented with 300 nM MLN4924 followed by 5 days in differentiation medium (5d MLN/5d diff.). Cells were stained with antibodies against pan-sarcomeric myosin heavy chain (MyHC) and desmin. DAPI was used as counterstain. Scale bar represents 100 μm. (B) Quantitative analysis of fusion index of differentiated C2C12 cells as in (A), compared to average fusion index of differentiated C2C12 cells after 5 days in culture (5d DMSO-CTL). Shown are averages and standard errors. Sample sizes and *p*-values are indicated in the figure. (C) Immunoblot analysis of whole cell lysates of C2C12 cells differentiated for 5 days with MLN4924, followed by 5 days of differentiation in medium (5d/5d), compared to MLN4924-treated (MLN) and vehicle-treated control (CTL, DMSO) cells differentiated for 10 days. Shown are representative immunoblots stained with antibodies against pan-sarcomeric MyHC and nedd8. GAPDH was used as loading control. (D) Quantitative analysis of MyHC protein levels [as in (C)].

reversible *in vitro*. The investigation of MyHC expression levels further substantiated that a recovery of C2C12 differentiation upon the removal of MLN4924 is evident. MyHC protein levels in C2C12 cells treated for 5 days with MLN4924 and subsequently left to recover in the normal differentiation medium showed comparable MyHC expression to differentiated control cells (Fig. 6C and D).

MLN4924-mediated blockage of the terminal myogenic differentiation program is partially overcome by removing epigenetic DNA modifications

Recently, a zinc finger and Bric-a-Brac, Tramtrack, Broad-complex (BTB)-domain-containing protein, ZBTB38 (CIBZ), were shown to be important for the initiation of the myogenic program [36]. ZBTB38 acts as a transcriptional repressor for myogenin expression in proliferative C2C12 myoblasts. Its repressor function can be overcome by treating C2C12 cells with 5-aza-dC (Aza), which is a DNA-methylation inhibitor. DNA methylation is required for ZBTB38 binding to the myogenin promoter and the repression of myogenin expression [36]. We therefore wondered if additional treatment of C2C12 with Aza may overcome some of the inhibitory effects of MLN4924 on terminal muscle cell differentiation. Indeed, C2C12 cells differentiated in the presence of Aza and MLN4924 show elevated expression of alpha-actinin and increased occurrence of alpha-actinin-positive cells (Fig. 7A–C). Next, we asked whether Aza may indeed contribute to the release of the repression of the myogenin promoter by ZBTB38 in the presence of MLN4924. Quantitative PCR analysis of Aza-treated C2C12 cells in the presence of MLN4924 shows a slight but significant increase of myogenin expression compared to C2C12 cells in the presence of MLN4924 alone (Fig. 7D). In fact, MLN4924-treated C2C12 show levels of myogenin transcripts similar to those found in proliferating myoblast cultures.

The increase in myogenin expression may explain how the Aza treatment of differentiating C2C12 in the presence of MLN4924 is able to overcome some of the inhibitory effects on muscle differentiation and may result in the increased mRNA and protein levels of alpha-actinin (Fig. 7A–C) and MyHC without affecting nedd8 expression (Fig. 7E).

The fusion index was also improved by the treatment with Aza (Fig. 7F), and the number of myotubes with >4 nuclei was increased compared to MLN-treated cells (Fig. 7G).

Protein levels of myogenic repressors Bhlhe41 and Id1, but not that of ZBTB38, are mediated through the activity of cullin E3-ligases

In an attempt to determine molecules that might be responsible for the failure to enter into the terminal myogenic differentiation program in cells deprived of cullin activity, we decided to focus on transcriptional factors important for differentiation. Interestingly, several transcriptional repressors of myogenesis are robustly expressed in proliferating myoblasts and decrease on the protein level within 24 h after the start of differentiation. Among them, ZBTB38 (CIBZ), Bhlhe41, and Id1 represent potential CRL substrates, because they either contain a BTB domain that indicates their interaction with cullin-3 [37,38], or due to the regulation of their degradation [39], or because of their known interaction with a cullin substrate adaptor [40,41]. While ZBTB38 protein levels are downregulated during differentiation, its mRNA levels remain unchanged throughout differentiation [36,42] (Supplementary Fig. S2A). In addition, the differentiation-dependent loss of ZBTB38 on the protein level can be blocked by the proteasome inhibitor MG132, indicating that the ubiquitin–proteasome pathway is actively regulating ZBTB38 protein levels [42]. In contrast, both Id1 and Bhlhe41 are decreased on the transcriptional and the protein level in differentiating myoblasts [39,43].

ZBTB38 contains a BTB domain, whose function poises the protein for interaction with the cullin-3-based E3-ubiquitin ligase [37,38]. We asked therefore whether the effect of MLN4924 on myoblast differentiation might be linked to this protein and its regulated degradation by cullin-3. We analyzed ZBTB38 protein levels in differentiating C2C12 cells in the presence of MLN4924 and in combination with Aza (Fig. 8A). While ZBTB38 protein levels decrease significantly during differentiation, a finding that has been reported previously [36,42], treatment with MLN4924, was unable to block its active degradation. Intriguingly, however, the additional incubation with Aza was consistently able to restore ZBTB38 protein levels comparable to those in proliferative C2C12 cells.

The fact that MLN4924 treatment was unable to prevent the degradation of ZBTB38 indicates that cullin E3-ligases, and more specifically a cullin-3-based E3-ligase, may not responsible for its poly-ubiquitylation and subsequent degradation. To ultimately rule out the putative involvement of cullin-3 for ZBTB38 degradation, we investigated whether both proteins are able to associate in co-immunoprecipitation (CoIP) and pull-down assays. No interaction was found either when probing the interaction with endogenous proteins from differentiating C2C12 cells (Fig. 8B) or when using the purified ZBTB38 BTB domain in combination with C2C12 protein lysates (Fig. 8C). A possible mechanism of how ZBTB38 levels might be regulated is found when we investigate changes to the subcellular localization of the protein during skeletal muscle differentiation. We observed a marked shift from a predominantly nuclear localization of ZBTB38 in proliferating C2C12 cells to a predominantly cytoplasmic localization in differentiated C2C12 cells (Fig. 8D), a mechanism that has been also observed for the degradation of Id1 [39]. We further investigated if MLN4924 treatment disrupted this shift in subcellular localization and found significant differences between MLN-treated and control cells 2 days after differentiation, indicating that cullin-based E3-ligases might indirectly be responsible for the
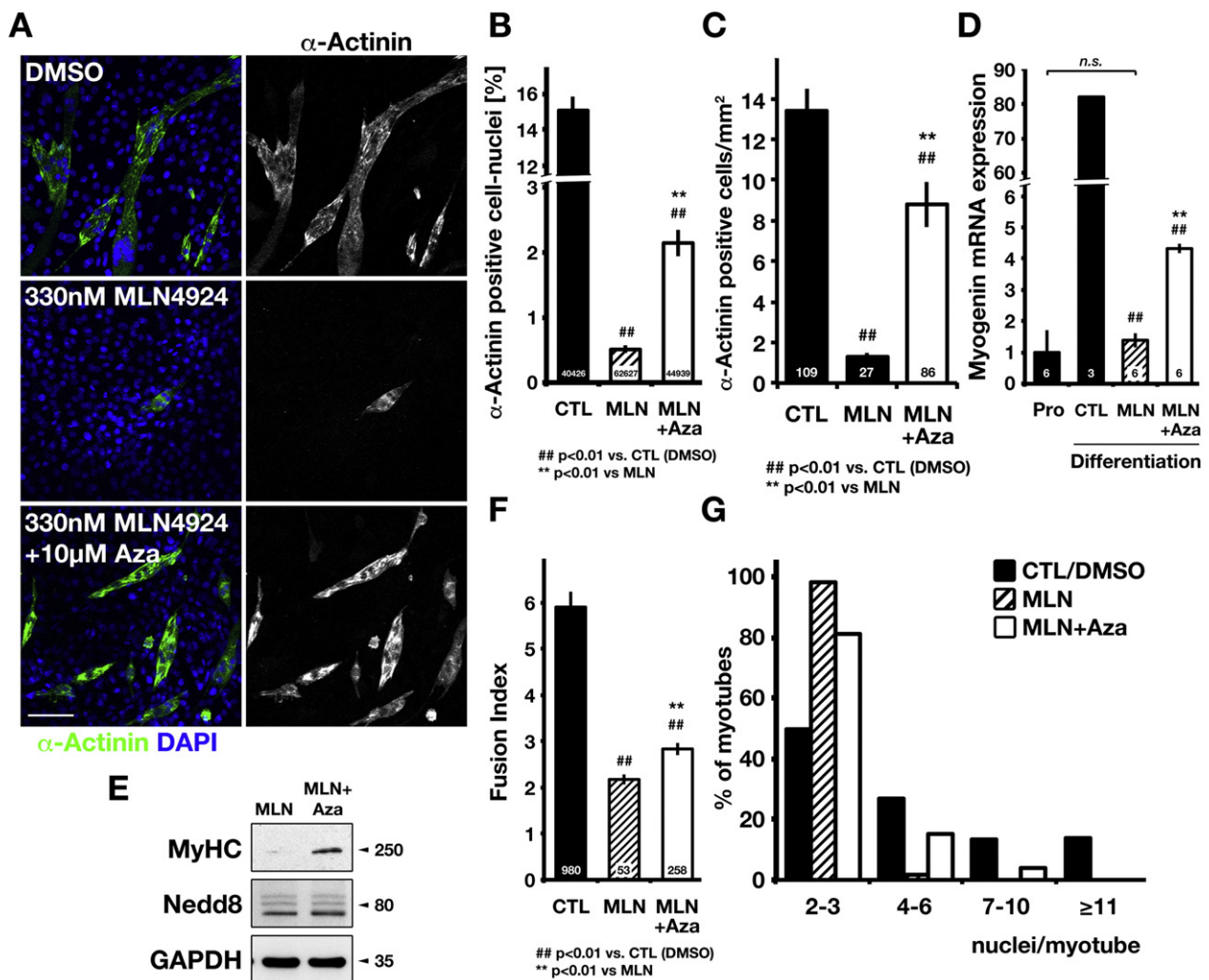
Fig. 7. 5-aza-dC (Aza) partially alleviates the inhibitory effects of MLN4924 on terminal C2C12 differentiation. (A) Immunofluorescence of C2C12 cells 5 days after differentiation in the presence of 330 nM MLN4924 alone and in combination with 10 µM Aza or vehicle control (DMSO). Cells were stained with an antibody against alpha-actinin (green in overlay). DAPI (blue in overlay) was used as counterstain. Scale bar represents 100 µm. (B) Fraction analysis of nuclei per alpha-actinin positive cells in 330 nM MLN4924 (MLN)-treated or 330 nM MLN4924- and 10 µM Aza-treated C2C12 5 days after differentiation, compared to vehicle control (CTL/DMSO). Sample size (total counted nuclei) and *p*-values are indicated in the figure. (C) Analysis of alpha-actinin positive cells per mm^2 in the presence of MLN4924 (MLN) alone, in combination with 10 µM Aza, or in control (CTL). Sample size of alpha actinin positive cells and *p*-values are indicated in the figure. (D) Quantitative PCR analysis of relative normalized (against GAPDH) myogenin expression in proliferative C2C12 myoblasts cultures (Pro), compared to C2C12 differentiated for 5 days in the presence of 330 nM MLN4924 (MLN) alone, in combination with 10 µM Aza, or in vehicle-treated control (CTL, DMSO). Sample size (biological replicates) and *p*-values are indicated in the figure. (n.s. = non-significant). (E) Immunoblot analysis of sarcomeric myosin heavy chain (MyHC) and nedd8 protein levels in differentiated C2C12 cells after 5 days in culture. Samples are total protein lysates of cells treated with 330 nM MLN4924 (MLN) alone or in combination with 10 µM Aza. (F and G) Fusion index (F) and cluster analysis of nuclei/myotube (G) of 330 nM MLN4924 (MLN)-treated or 330 nM MLN4924- and 10 µM Aza-treated C2C12 5 days after differentiation, compared to vehicle control (CTL/DMSO). Sample size and *p*-values (in F) are indicated in the figure.

nuclear exclusion of ZBTB38, but not for its direct degradation (Supplementary Fig. S2B and C).

In contrast to ZBTB38, MLN4924 treatment of differentiating myoblasts increases both Id1 and Bhlhe41 protein but not mRNA levels 2 days after the start of differentiation when compared to untreated control cells, which demonstrate a marked loss of these proteins (Fig. 8E and Supplementary Fig. S2D). In summary, our data indicate that cullin-based E3-ligases might be responsible for the degradation of myogenic repressors Id1 and Bhlhe41, but not that of ZBTB38.
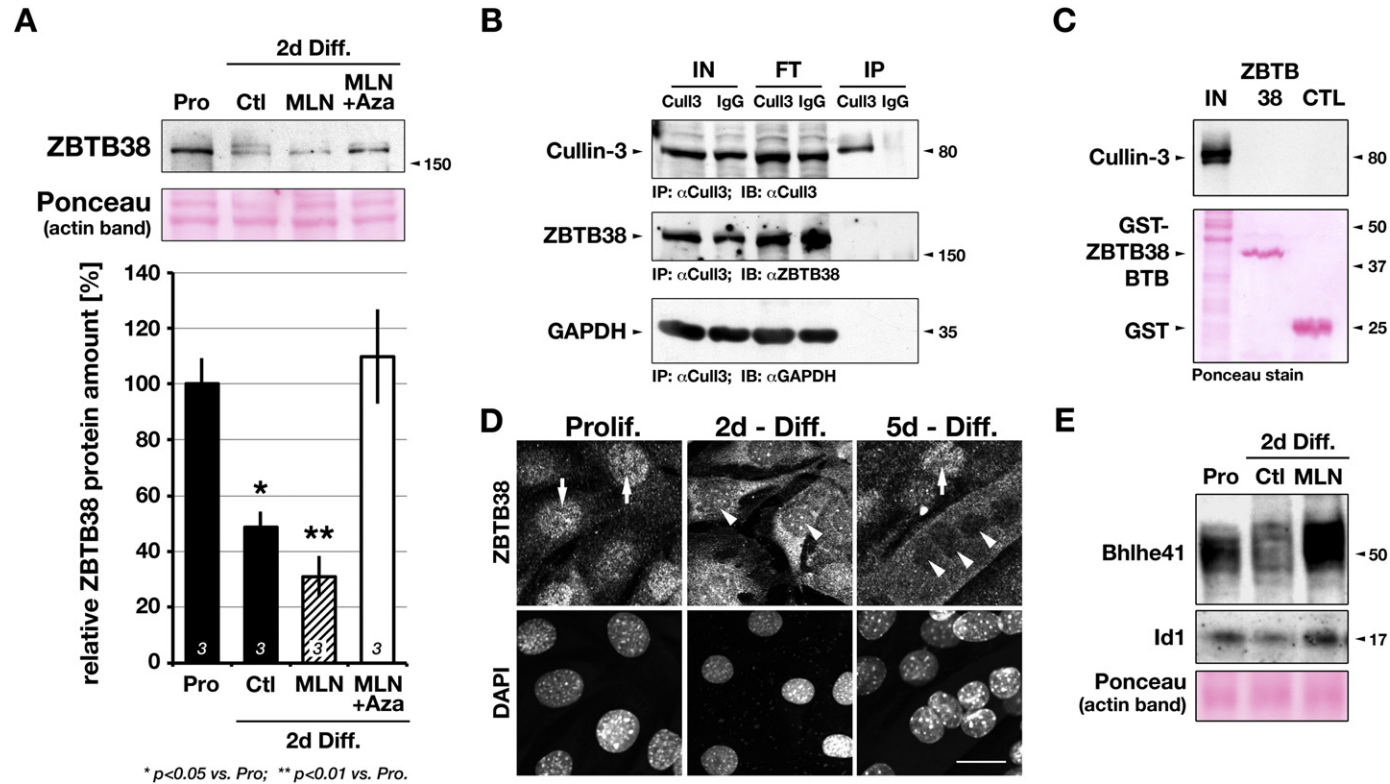
Fig. 8. Analysis of protein degradation of myogenic repressors ZBTB38, Bhlhe41, and Id1. (A) Analysis of ZBTB38 protein levels in C2C12 cells during proliferation or 2 days after differentiation in the presence of DMSO (Ctl), 330 nM MLN4924 (MLN), or 330 nM MLN4924 (MLN) and 10 μM 5-aza-dC (Aza). Ponceau was used to demonstrate equal loading. Shown are a representative immunoblot (upper panel) and the quantification of protein levels (lower panel). Sample size and *p*-values are indicated in the figure. (B and C) Analysis of protein interaction between cullin-3 and either full-length ZBTB38 in a CoIP experiment (B) or the BTB domain of ZBTB38 only in a GST-pull-down experiment (C) indicates no association between the two proteins. GAPDH and normal rabbit-IgG were used as controls in (B). GST alone was used as control in (C). Abbreviations: IN, Input; FT, flow-through; IP, immunoprecipitate; CTL, control. (D) Analysis of subcellular ZBTB38 distribution during proliferation and differentiation at 2 and 5 days in C2C12 cells. Cells were stained with an antibody against ZBTB38 and labeled with DAPI to outline nuclei. Arrows indicate primarily nuclear and localized ZBTB38 in proliferative and undifferentiated C2C12 cells, whereas arrowheads point to nuclei of differentiated C2C12 cells. Scale bar represents 50 μm. (E) Analysis of Bhlh41 and Id1 protein levels during proliferation (Pro) and 2 days after the onset of differentiation (Diff.) in the presence (MLN) or absence (Ctl) of MLN4924. Ponceau staining of total proteins (actin band) was used as loading control.

Discussion

Cullin functions for terminal muscle cell differentiation

The differentiation process from the pluripotent progenitor stem cell to skeletal muscle stem cells (satellite cells), into functional skeletal muscles, which are anchored and organized into muscle–tendon units, underlies a complex system of biological steps and developmental milestones (Fig. 9). Each of those steps is characterized by the change in the genetic program that is derived by the induction of muscle-specific transcription factors like MyoD or myogenin (and the disappearance of proliferation markers like PCNA [45,46]) and the expression of characteristic muscle proteins or differentiation "milestones", like myoblast fusion, the formation of the neuromuscular junction, or muscle innervation. The premise of our experiments was to delineate the role that cullin-based E3-ligases play for the early steps in the terminal skeletal muscle cell differentiation program. The role for various cullin E3-ligase substrate adaptors during muscle atrophy and various forms of skeletal muscle myopathy is very well investigated. Specifically, the functions of the cullin-1-specific substrate adaptor atrogin-1 (MAFbx, Fbxo32) [10], and more recently through cullin-3 interacting substrate adaptors [11,47,48], are well characterized. However, investigations into the biological functions of cullin E3-ligases activity during muscle cell differentiation are largely lacking.

By using the C2C12 skeletal muscle cell line, and the small inhibitor MLN4924 that acts downstream of the Nae1 E1-enzyme on cullin activity, we were able to tease out the role for this class of ubiquitin ligases for three of the crucial steps during skeletal muscle differentiation: commitment to the terminal myogenic differentiation program, myoblast fusion, and AChR clustering.

Commitment to the terminal myogenic differentiation program

The requirement of cullin activity for the entry into the terminal myogenic differentiation program is one of the major findings of our study. Reasoning that cullin-mediated E3-ligase function may be required for the degradation of an inhibitory factor/repressor for myogenic transcription factors, we screened for proteins that are known to be degraded by cullin-based ubiquitin ligases, interact with a protein that contains one of the known cullin substrate adaptor domains (e.g., F-box domain, VHL-box domain, BTB/POZ domain, or SOCS domain), or is a protein that itself incorporates a cullin substrate adaptor domain.

A multitude of proteins have been shown to act as a repressor for the entry into the myogenic program.

Examples include ATBF1-A (ZFHX3) [49], Id1 [50,51], Teashirt-3 [52], Hey-1 [53], HMGA1 [54], the MBD2-interacting zinc finger protein MIZF [55], Staufen1 [56], JAZF1 [57], Foxk1 [58], Bhlhe41 (DEC2, Sharp1) [43], or ZBTB38 (CIBZ) [36,42]. Little is known about any association of these proteins to cullin-linked protein degradation. Only Bhlhe41 was shown to interact with Fbxw11 (beta-TRCP2) [40], a known substrate adaptor for cullin-1 [41], thereby indicating that this basic helix-loop-helix transcription factor may be degraded in a cullin-dependent way. Although Id1 and ZBTB38 have been shown to be degraded through the ubiquitin proteasome system [39,42], it remained unclear if cullin E3-ligases play a role in their degradation. However, the zinc finger protein ZBTB38 contains a BTB domain, predisposing the protein to interact with cullin-3 [37,38]. Hence, we decided to focus on these three repressor proteins and investigated if the loss of their regulated degradation in the absence of CRL activity could be responsible for the lack of terminal muscle cell differentiation.

Our data show that ZBTB38 protein degradation is not regulated through a cullin E3-ubiquitin ligase-dependent mechanism and that the protein does not associate with cullin-3. Thereby, our data add for the first time ZBTB38 to the short list of BTB domain proteins that were recently shown to not bind to cullin-3 [59,60].

We also investigated Bhlhe41 and Id1 protein levels, which are found to be decreased during differentiation. Treatment with MLN4924 led to their accumulation, with protein levels similar or in excess to the undifferentiated state of C2C12 cells, thus indicating that both myogenic repressors are potential targets for cullin-mediated protein degradation.

An unexpected finding of our experiments to reverse the MLN4924-induced blockage of terminal skeletal muscle differentiation was that the addition of 10 µM Aza to the medium enhanced ZBTB38 protein levels. Aza has been shown to induce ubiquitin C-terminal hydrolase L1 (UCHL1), a de-ubiquitylating enzyme [61], thereby promoting the stability of poly-ubiquitylated substrate proteins. This mechanism might be responsible for the observed increase in ZBTB38 protein levels. Intriguingly, UCHL1 protein levels are decreased during muscle differentiation [62] but can be elevated in atrophic muscles [63,64]. UCHL1 was also required to maintain the structure of the NMJ, although not in the postsynaptic muscle, but in the presynaptic nerve [65].

Myoblast fusion

Myoblast fusion is another important step during skeletal muscle differentiation. The fusion process has been shown to involve cell migration, cell
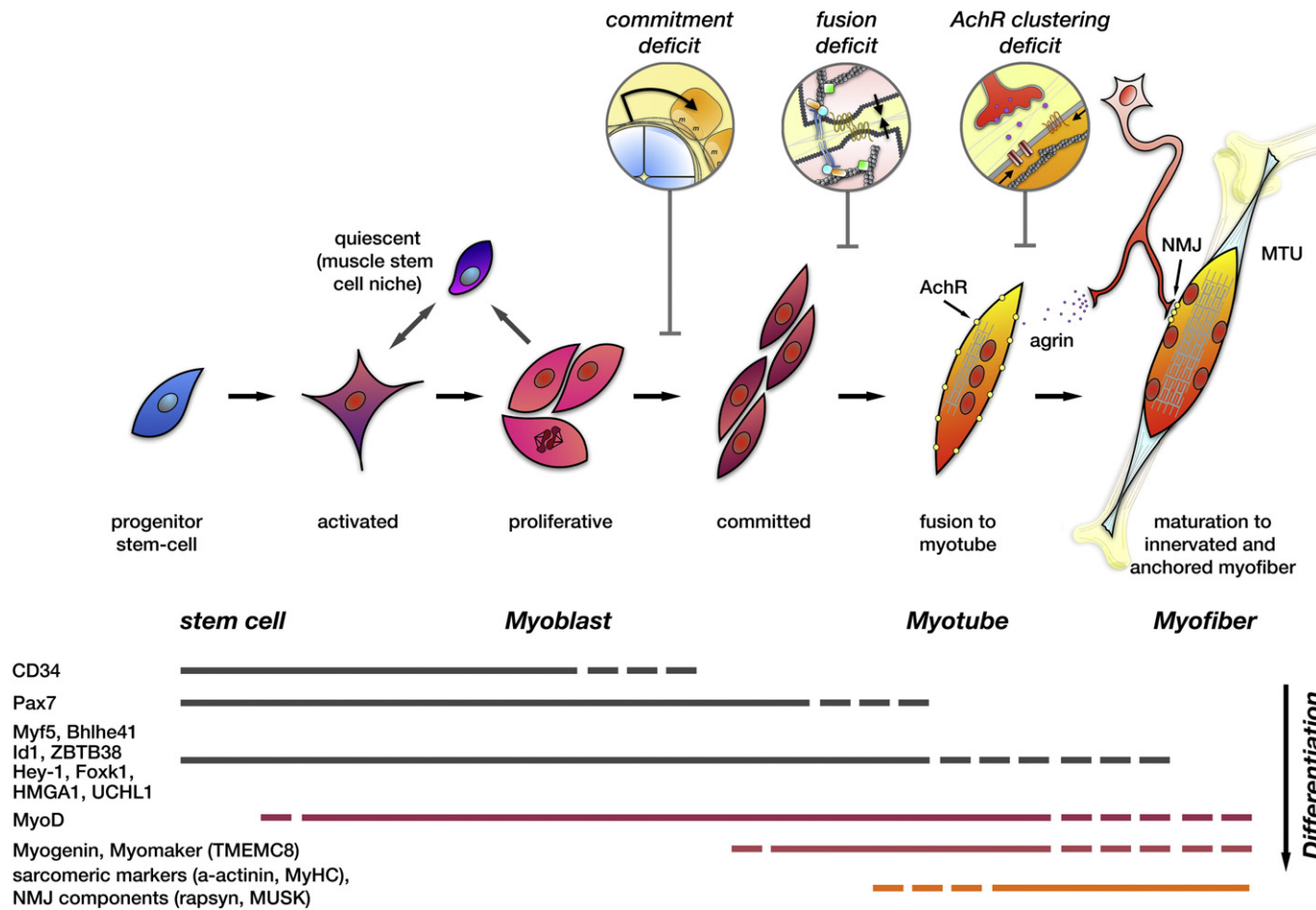
Fig. 9. Cullin requirement in the terminal skeletal muscle differentiation process. Overview of biological steps and developmental milestones for the differentiation from pluripotent progenitor stem cells, to skeletal muscle stem cells (satellite cells), into skeletal muscle myofibers that are anchored by tendons (muscle–tendon unit; MTU). Shown are marker genes and their approximate temporal expression during the differentiation process. Effect of cullin E3-ubiquitin ligase inhibition for each of the differentiation steps is indicated. Figure adapted from Ref. [44].

recognition and adhesion, cytoskeletal remodeling, fusion-related activation of signaling pathways, and assembly and activation of proteins that make out the "fusion machinery", which leads to membrane remodeling and ultimately the fusion of the differentiating myoblasts (for a review, see Refs. [66,67]). We noted in our timed inhibitor experiment (Fig. 1E–G) and in the experiments involving Aza (Fig. 7A–C and F) a lack of myoblast fusion.

Specifically, the addition of MLN4924 after 3 days of differentiation still leads to a pronounced defect in the fusion index (Fig. 1F), when compared to control cells, despite the fact that the expression of many transcription factors necessary for terminal muscle differentiation (e.g., myogenin [68]), and the proteins that are involved in the fusion of myoblasts (e.g., myomaker (TMEM8C) [69]), already peak at this stage during myotube development and hence should not be affected by the inhibition of CRL functions. Moreover, in our experiments involving Aza, we also noticed a lack of expected myoblast fusion. This is mostly based on the discrepancy between alpha-actinin positive cells after the additional treatment with Aza (Fig. 7C), which leads to a more pronounced increase, compared to the measured increase in the fusion index (Fig. 7F). This discrepancy might be attributed to a defect in myotube fusion that is not overcome by Aza treatment.

AChR clustering

NMJ development and formation rely on AChR clustering. *In vivo*, this developmental step is dependent on signaling molecules coming from both presynaptic (i.e., neural agrin) and postsynaptic (i.e., MusK, Rapsyn) elements [70]. Recently, data revealed that neddylation is involved in synapse structure and maintenance in hippocampal neurons [71]. However, the effect of the loss of CRL activity on the postsynaptic element of neuromuscular junction has never been investigated. *In vitro*, AchR clustering can be induced by treating myotubes with neural agrin [72]. Our data indicate that agrin-induced AChR clustering is impaired in the absence of cullin activity. Interestingly, Rpy-1, the ortholog of Rapsyn in *Caenorhabditis elegans*, can be degraded by a CRL [73], suggesting unexplored functions for CRLs and their substrates in the formation of NMJ. Our data indicate that a defective ubiquitylation activity through CRL inhibition might interfere either with the abundance of proteins that are important for neuromuscular junction development or with cytoskeletal remodeling that has been shown to be important for the agrin-induced AchR clustering process [74–79]. Indeed, several members of the cullin protein family associate with and are capable of remodeling actin and tubulin filaments in non-muscle cells [80–84]. The biological function of these CRLS at the cytoskeleton may also extend to myoblasts, as we find cullin-3 associated with the tubulin cytoskeleton in skeletal muscle myoblasts (Supplementary Fig. S3). Further investigation will be needed to understand the importance of the turnover regulation of proteins involved in synaptogenesis and NMJ formation [70].

Clinical implications for cullin inhibition

Unexpectedly, this study also brings up a potential therapeutic concern for patients treated with MLN4924. Cullin-based E3-ubiquitin ligases play a major role for cell survival and signaling. Indeed, most of the biological roles for cullin-based E3-ubiquitin ligases have been assigned to fundamental functions like their critical involvement in the cell cycle, apoptosis, cell migration, or cell proliferation. These attributes have made cullin proteins an attractive anticancer target [14,17,85–87]. While CRL functions can be disrupted in many ways, MLN4924 (Pevenedistat) has emerged as one of the first compounds to be tested in phase I clinical trials, as it is effective against a variety of cancers and is able to inhibit the entire family of cullin-based ubiquitin ligases [85]. Although the concentrations and administration regiments used for tests in mice and in clinical trials vary, dosages of up to 150 mg/kg have been reported [33], which equal to a "global" MLN4924 concentration of approximately 350 μM for the average mouse with a weight of 40 g, or a human with a weight of 69 kg. Data from our dose–response curve (Fig. 2B) indicated that the IC_{50} of MLN4924 on the C2C12 myotube fusion index is approximately 100 nM, more than 3 magnitudes lower than the approximate concentration achieved *in vivo*. Although our IC_{50} value on the fusion index of ~ 100 nm is 25 times higher than the reported IC_{50} of NAE1 itself, it is at least 10 times lower than MLN4924 inhibition of NAE1-related enzymes UAE, SAE, UBA6, or ATG7 [14]. The measured IC_{50} of MLN4924 on the fusion index indicates that the observed effects are likely due to the inhibition of NAE1 and the subsequent suppression of cullin E3-ligase activity, and not the off-target effects of NAE1-related enzymes. This finding is also supported by our siRNA experiment that specifically inhibits cullin activation through the knockdown of nedd8 (Fig. 2D and E).

Numerous cancer patients develop a pathological muscle loss, a symptom associated with the cachexia syndrome. Cachexia is estimated to be responsible for the death of 20% of patients with cancer [22]. A recent study revealed that muscle regeneration and satellite cell differentiation are affected in cachectic mice and that defective myogenesis may participate in muscle wasting observed in patients [23]. For the first time, we show that MLN4924, a drug used in clinical studies for cancer therapy, may interfere with the terminal muscle cell differentiation *in vitro*. If validated *in vivo*,

a synergistic effect of MLN4924 over the myoblast differentiation program combined with the satellite cells defect observed in cachectic patients [22,23] would be detrimental. It seems essential to closely monitor the skeletal muscles of patients treated with MLN4924 in future studies.

Material and Methods

C2C12 and primary myoblast cell culture and reagents

C2C12 cells were grown in Dulbecco's modified Eagle's medium (Corning Life Sciences, Tewksbury, MA) containing 4.5 g/l glucose, supplemented with 15% fetal bovine serum (FBS; Gemini Bio-Products, Sacramento, CA) and penicillin-streptomycin (Cellgro). Cells were maintained at 37 °C in a saturated humidity atmosphere containing 5% CO_2. Differentiation of C2C12 myoblasts was triggered when cells reached 70% of confluency by replacing FBS with 2% horse serum (HS; Lonza BioWhittaker, Basel, Switzerland). The fusion index was calculated as the mean number of nuclei per myotube at day 5 of differentiation. Myotubes were defined as sarcomeric MyHC or alpha-actinin positive cells containing at least 2 nuclei.

Mouse primary myoblasts were obtained by the dissection of hind limb muscles from 1-month-old mice. Muscles were digested in Collagenase B-Dispase II (Roche, USA) solution for 30 min at 37 °C. Cell suspension was filtered through a 75 -μm cell strainer, pelleted via centrifugation, resuspended in Ham's complete medium (Ham's F-10 media, Corning Life Sciences, Tewksbury, MA), 20% FBS, 2% penicillin-streptomycin (Cellgro) and bFGF (5 ng/mL; Invitrogen, Carlsbad, CA), and pre-plated on uncoated dish for 2 h at 37 °C with 5% CO_2. Supernatant was collected and plated on 0.2% gelatin (Sigma, Saint-Louis, MO)-coated dish, and cells were incubated at 37 °C with 5% CO_2. Ham's complete medium was refreshed every 2 days. Differentiation of cells was achieved with 2% HS (Lonza BioWhittaker, Basel, Switzerland).

MLN4924 compound was purchased from Life-Sensors, Inc. (Malvern, PA) and redissolved in DMSO, and stock solution was stored at a concentration of 1 mM at −20 °C. Aza was purchased from Fisher Scientific and redissolved in DMSO. Working solutions were prepared by dilution of stock solution into culture media. Media with inhibitors were refreshed every 48 h. Control cells were treated with a corresponding concentration of DMSO (Sigma-Aldrich).

We purchased a 90-KDa recombinant rat agrin compound from R&D Systems (Minneapolis, MN) and reconstituted it in sterile phosphate-buffered saline (PBS) containing 0.1% BSA. AChR clustering was induced by overnight incubation with 5 ng/mL recombinant rat agrin.

siRNA

Proliferating C2C12 cells were transfected with siRNA directed against nedd8 [ON-TARGETplus mouse nedd8 (18002) individual siRNA; GE Healthcare Dharmacon] or scrambled control (ON-TARGETplus non-targeting siRNA #1; GE Healthcare Dharmacon) using DharmaFECT 1 transfection reagent (GE Healthcare Dharmacon) according to the manufacturer's instructions. Then, 24 h after transfection, cells were changed into differentiation medium and allowed to proliferate for 3 or 5 days before analysis.

Isolation and culture of human myoblasts

Human satellite cells were enzymatically isolated from semitendinosus and gracilis muscle biopsies obtained from typically developing children ($n = 8$ patients, 16.4 ± 1.6 years old). The University of California San Diego Human Research Protection Program provided ethical approval, and appropriate assents/consents were obtained from children and their parents. Satellite cells were isolated by enzymatic procedures as previously described [88]. Briefly, satellite cells were isolated by sequential digestion in a Collagenase B–Dispase II solution (Roche) at 37 °C and resuspended in fluorescence-activated cell sorting buffer before being sorted by flow cytometry. Satellite cells were sorted from other cell populations using specific cell surface markers and were defined as a population of CD31−/CD45−/CD56+/ITGA7+ mono-nucleated cells, as previously published [89]. Satellite cell-derived myoblasts were expanded *in vitro* in Ham's F-10 medium (Corning Life Sciences, Tewksbury, MA), supplemented with 20% FBS and 2% penicillin-streptomycin (Cellgro) and bFGF (5 ng/mL; Invitrogen, Carlsbad, CA) on 0.2% (porcine) gelatin-coated dishes. To stimulate fusion and myotubes formation, we switched the medium to a low-serum medium containing Dulbecco's modified Eagle's medium (1 g/L glucose) and 2% HS (Lonza BioWhittaker, Basel, Switzerland) when myoblasts reached 60–70% confluence.

Cloning and protein purification

The murine version of the ZBTB38 BTB domain (accession number: NM_175537) was subcloned in frame to the glutathione *S*-transferase (GST)-C1 vector [90] using murine skeletal muscle cDNA as a template and standard PCR conditions with the following oligonucleotides: ZBTB38-BTB.fwd: CCGCTCGAGC CACCATGACAGTCATGTCCCTCTCC and ZBTB38-BTB.rev: GGAATTCGAGGACCTGGGGAATTTGAG.

The construct was subsequently verified for correct integration by sequencing.

Expression of the GST-tagged BTB domain of ZBTB38 or GST alone was done by transforming BL21 cells (C601003; Invitrogen; ThermoFisher Scientific) and growing them in 400 ml of LB medium supplemented with 50 µg/ml carbenicillin on an orbital shaker at 37 °C to an OD_{600} of >600. Expression of the GST-fusion protein or GST alone was induced by the addition of 0.2 mM IPTG and performed for approximately 12 h at 18 °C. Cells were pelleted and lysed into 40-ml ice-cold lysis buffer [150 mM NaCl, 10 mM Tris–HCl (pH 8) 1% Triton X100], followed by sonication for 1 min at 4 °C and 70% output (Vibracell, Sonics & Materials Inc., Newtown, CT). Insoluble cell debris was removed by centrifugation (45 min at 11,000 rpm, 4 °C; Sorvall), and the supernatant was incubated with 400 µl glutathione-Sepharose beads (bioPLUS fine research chemicals) for 2 h at 4 °C with agitation. After the washing of beads with ice-cold PBS for three times, bound protein was eluted with GST elution buffer [150 mM NaCl, 50 mM Tris–HCl (pH 7.4), and 150 mM reduced glutathione] and dialyzed overnight at 4 °C against dialysis buffer [20 mM Hepes-KOH (pH 7.4), 10 mM MgSO4, and 0.1 mM CaCl2].

Protein interaction assays

To test for the interaction of proteins, we employed either GST-pull-down assays as described previously [90] or CoIP assays.

For CoIP and pull-down assays, confluent cultures of differentiating C2C12 cultures (2 days after differentiation start) were lysed into ice-cold lysis buffer [150 mM NaCl, Tris–HCl (pH 8), 1 mM DTT, 1x Complete Protease Inhibitor EDTA-free (Roche), 1x PhosSTOP (Roche), and 0.2% NP-40]. Insoluble cell debris was removed by centrifugation at 14,000 rpm at 4 °C for 10 min. For GST-pull-down assays, cell lysates were incubated with 2 µg of either GST-ZBTB38 (BTB domain) or GST alone for 2 h at 4 °C on a rotating shaker, followed by the addition of 20 µl glutathione-Sepharose beads (bioPLUS fine research chemicals) and additional incubation for 1 h. Beads were washed three times with ice-cold PBS, and bound proteins were analyzed by SDS-page following immunoblot analysis. For CoIP, cell lysates were precleared using G-protein-linked magnetic beads (Dynabeads; ThermoFisher Scientific) for 1 h at 4 °C on a rotating shaker. After preclearing, lysates were incubated with 1 µg of primary antibody or control serum for 2 h at 4 °C. After the addition of G-protein-linked magnetic beads (Dynabeads), lysates were incubated on a rotating shaker at 4 °C for an additional hour and centrifuged, and beads were washed three times with ice-cold PBS. After the last wash, PBS solution was removed, and bound proteins were

eluted off the beads using SDS sample buffer. Samples were analyzed using SDS-page, followed by immunoblot analysis.

Extraction of total RNA, RT-PCR, and RT-qPCR analysis

Cells were washed with PBS and then lysed using TRIzol reagent (ThermoFisher Scientific). RNA was extracted according to the manufacturer's instructions. Purity of RNA was assessed by a ratio of absorbance at 260 nm and 230 nm >1.7. Then, 200 ng of RNA was used for reverse transcriptase reaction using the Maxima First Strand cDNA Synthesis kit (Fermentas; ThermoFisher Scientific) and random hexamers. Oligonucleotides optimized for qPCR of murine myogenin (myogenin.fwd: CTACAGGCCTTGCT CAGCTC; myogenin.rev: AGATTGTGGGCGTCTG TAG), GAPDH (GAPDH.fwd: GCTCATGACCA CAGTCCATG ; GAPDH.rev: GAAGGCCATGCCA GTGAGC), cyclophilin B (cycloB.fwd: GATGGCA CAGGAGGAAAGAG; cycloB.rev: AACTTTGCC GAAAACCACAT), nedd8 (nedd8.fwd: TCTACAGT GGCAAGCAAATGA; nedd8.rev: TTTCTTCAC TGCCCAAGACC), Id1 (Id1.fwd: GCGAGATCAGTG CCTTGG; Id1.rev: CTCCTGAAGGGCTGGAGTC), and ZBTB38 (ZBTB38.fwd: AGGCTGGCGTGTTCT GAG; ZBTB38.rev: CACTGTGAAAGTCGTCCTT GAG) were used in reactions employing the PerfeCTa SYBR green real-time PCR mix (Quanta BioSciences; Beverly, MA) and a CFX96 thermocycler (BioRad; Hercules, CA). Samples were normalized to either GAPDH or cyclophilin B. If not noted otherwise, three biological samples were analyzed per sample group.

Immunofluorescence microscopy

Cells were rinsed one time with PBS, fixed for 15 min with 4% paraformaldehyde, and rinsed three times with PBS. For the labeling of mitochondria, cells were incubated with fluorescently labeled MitoTracker (ThermoFisher Scientific) according to the manufacturer's instructions before fixation. Cells were then permeabilized for 10 min in 1xPBS supplemented with 0.2% Triton X-100 (Sigma Aldrich; St. Louis, MO), washed three times with PBS, and incubated in blocking solution [Gold Buffer (150 mM NaCl and 20 mM Tris (pH 7.4) supplemented with 1% BSA] for 1 h at room temperature before incubation with primary antibodies against pan-sarcomeric MyHC (clone 1025, DSHB), alpha-actinin (clone EA-53, VWR), Desmin (Santa Cruz Biotechnology; Dallas, TX), ZBTB38 (R&D Systems; Minneapolis, MN), myogenin (clone F5D), beta-tubulin (clone E7, DSHB), or MYH7 (clone BA-D5, DSHB) diluted in blocking solution. Primary antibodies were incubated for either 2 h at room temperature or overnight at 4 °C. Following incubation, cells were washed three times for 5 min with PBS and incubated with secondary antibodies (all from Jackson Immuno

Research Laboratories Inc.; West Grove, PA) diluted into blocking solution for 1 h at room temperature. Secondary antibody mixtures also contained 4′, 6′ diamidino-2-phenylindol (DAPI) and/or fluorescently linked alpha-bungarotoxin (Molecular Probes, ThermoFisher Scientific), Alexa Fluor 488 conjugate of wheat germ agglutinin (ThermoFisher Scientific), or fluorescently labeled phalloidin (Molecular Probes; ThermoFisher Scientific) when appropriate. After washing three times with PBS for 5 min, cells were mounted using fluorescent mounting medium (Dako; Carpinteria, CA). Microscopy was performed using an Olympus FV1000 confocal microscope using the $20\times$ air objective, the $40\times$, or $63\times$ oil immersion objective and zoom rates between 1 and 3 in sequential scanning mode.

Evaluation of fluorescent cytoplasmic *versus* nuclear ZBTB38 localization ratios was done as described previously [71], using ImageJ (1.48v) [91] and Excel.

Staining and quantification of AChRs in C2C12 myotubes

After 5 days of differentiation, myotubes were treated with MLN4924 compound or DMSO for 1 day and then incubated with recombinant rat agrin overnight at 37 °C in 5% CO2. Treated cells with recombinant rat agrin were fixed in 4% paraformaldehyde (PFA) for 10 min. Quantification of AChR expressed at the myotubes surface was determined by incubating fixed cells with fluorescein isothiocyanate (FITC) conjugated alpha-bungarotoxin (Molecular Probes, ThermoFisher) for 1 h at room temperature. Confocal microscopy was performed using a Zeiss Axioplan 2 upright confocal microscope (Carl Zeiss Inc., Thornwood, NY). Area, number, and size of AChR were assessed using ImageJ (1.48v) software [91].

Western blot analysis

Cells were washed in PBS and put in lysis buffer [150 mM NaCl, 50 mM Tris–HCl (pH 8), 0,1% Triton-100, 1x Complete EDTA-free protease inhibitor (Roche; Indianapolis, IN), and 1x PhosStop phosphatase inhibitor (Roche; Indianapolis, IN)] for 20 min on ice. Lysates were sonicated and spun for 10 min at 10,000g. After the quantification of protein concentration using Pierce BCA Protein Assay Kit (ThermoFisher Scientific; Whaltham, MA), 5 to 15 μg of clarified lysates was separated by SDS-PAGE. Transfer was performed on nitrocellulose membranes (BioRad). Membranes were incubated with blocking solution (TBS-Tween containing 5% BSA) for 1 h at room temperature and then incubated with antibodies against cullin1 (Sigma Aldrich; St. Louis, MO), cullin3 (Sigma Aldrich; St. Louis, MO, or gift from J. Singer), nedd8 (Cell Signaling; Danvers, MA), pan-sarcomeric MyHC (clone 1025, DSHB), myogenin (clone F5D, from DSHB and Abcam),

ZBTB38 (R&D Systems; Minneapolis, MN), Bhlhe41 (ARP33575; AVIVA Systems Biology, San Diego, CA), Id1 (sc-133,104; Santa Cruz Biotechnologies), or GAPDH (Santa Cruz Biotechnologies) in blocking solution overnight at 4 °C. After washing, secondary horseradish peroxidase (HRP) linked antibodies (DAKO, Cell Signaling) were applied for 1 h at room temperature. After washing, antibody-bound proteins were visualized on X-ray films. Quantification of band intensities was performed using ImageJ software (1.48v) [91].

Statistical analysis

Significance was assessed using the two-tailed student's *t*-test. Data are expressed as mean ± standard error of the mean, and differences were considered statistically significant if $p < 0.05$.

Accession numbers

The mouse ZBTB38 mRNA accession number type ID is NM_175537.

Supplementary data to this article can be found online at http://dx.doi.org/10.1016/j.jmb.2017.02.012.

References

[1] B. Blaauw, S. Schiaffino, C. Reggiani, Mechanisms modulating skeletal muscle phenotype, Compr. Physiol. 3 (2013) 1645–1687.

[2] M. Sandri, Protein breakdown in muscle wasting: role of autophagy–lysosome and ubiquitin-proteasome, Int. J. Biochem. Cell Biol. 45 (2013) 2121–2129.

[3] J. Blondelle, S. Lange, Cardiac cytoarchitecture: how to maintain a working heart—waste disposal and recycling in cardiomyocytes Chapter: 12 in: E. Ehler (Ed.) 1st edit., Cardiac Cytoarchitecture, Springer, Switzerland 2015, pp. 245–309.

[4] A.L. Goldberg, Protein degradation and protection against misfolded or damaged proteins, Nature 426 (2003) 895–899.

[5] P. Bonaldo, M. Sandri, Cellular and molecular mechanisms of muscle atrophy, Dis. Model. Mech. 6 (2013) 25–39.

[6] D.R. Bosu, E.T. Kipreos, Cullin–RING ubiquitin ligases: global regulation and activation cycles, Cell Div. 3 (2008) 7.

[7] M.D. Petroski, R.J. Deshaies, Function and regulation of cullin–RING ubiquitin ligases, Nat. Rev. Mol. Cell Biol. 6 (2005) 9–20.

[8] W. Zhou, W. Wei, Y. Sun, Genetically engineered mouse models for functional studies of SKP1-CUL1-F-box-protein (SCF) E3 ubiquitin ligases, Cell Res. 23 (2013) 599–619.

[9] T. Kamitani, K. Kito, H.P. Nguyen, E.T. Yeh, Characterization of NEDD8, a developmentally down-regulated ubiquitin-like protein, J. Biol. Chem. 272 (1997) 28,557–28,562.

[10] S.C. Bodine, E. Latres, S. Baumhueter, V.K. Lai, L. Nunez, B.A. Clarke, et al., Identification of ubiquitin ligases required for skeletal muscle atrophy, Science 294 (2001) 1704–1708.

[11] V.A. Gupta, A.H. Beggs, Kelch proteins: emerging roles in skeletal muscle development and diseases, Skelet. Muscle 4 (2014) 11.

[12] J. Lee, P. Zhou, Cullins and cancer, Genes Cancer 1 (2010) 690–699.

[13] S. Jackson, Y. Xiong, CRL4s: the CUL4-RING E3 ubiquitin ligases, Trends Biochem. Sci. 34 (2009) 562–570.

[14] T.A. Soucy, P.G. Smith, M.A. Milhollen, A.J. Berger, J.M. Gavin, S. Adhikari, et al., An inhibitor of NEDD8-activating enzyme as a new approach to treat cancer, Nature 458 (2009) 732–736.

[15] K. Nakayama, H. Nagahama, Y.A. Minamishima, M. Matsumoto, I. Nakamichi, K. Kitagawa, et al., Targeted disruption of Skp2 results in accumulation of cyclin E and p27(Kip1), polyploidy and centrosome overduplication, EMBO J. 19 (2000) 2069–2081.

[16] J.D. Singer, M. Gurian-West, B. Clurman, J.M. Roberts, Cullin-3 targets cyclin E for ubiquitination and controls S phase in mammalian cells, Genes Dev. 13 (1999) 2375–2387.

[17] Y. Zhao, Y. Sun, Cullin–RING ligases as attractive anti-cancer targets, Curr. Pharm. Des. 19 (2013) 3215–3225.

[18] J.J. Shah, A.J. Jakubowiak, O.A. O'Connor, R.Z. Orlowski, R.D. Harvey, M.R. Smith, et al., Phase I study of the novel investigational NEDD8-activating enzyme inhibitor Pevonedistat (MLN4924) in patients with relapsed/refractory multiple myeloma or lymphoma, Clin. Cancer Res. 22 (2016) 34–43.

[19] J. Sarantopoulos, G.I. Shapiro, R.B. Cohen, J.W. Clark, J.S. Kauh, G.J. Weiss, et al., Phase I study of the investigational NEDD8-activating enzyme inhibitor Pevonedistat (TAK-924/MLN4924) in patients with advanced solid tumors, Clin. Cancer Res. 22 (2016) 847–857.

[20] J.M. Argiles, S. Busquets, B. Stemmler, F.J. Lopez-Soriano, Cancer cachexia: understanding the molecular basis, Nat. Rev. Cancer 14 (2014) 754–762.

[21] S. Warren, The immediate causes of death in cancer, Am. J. Med. Sci. 184 (1932) 610–615.

[22] R.J. Skipworth, G.D. Stewart, C.H. Dejong, T. Preston, K.C. Fearon, Pathophysiology of cancer cachexia: much more than host–tumour interaction? Clin. Nutr. 26 (2007) 667–676.

[23] W.A. He, E. Berardi, V.M. Cardillo, S. Acharyya, P. Aulino, J. Thomas-Ahner, et al., NF-kappaB-mediated Pax7 dysregulation in the muscle microenvironment promotes cancer cachexia, J. Clin. Invest. 123 (2013) 4821–4835.

[24] C.M. Prado, J.R. Lieffers, L.J. McCargar, T. Reiman, M.B. Sawyer, L. Martin, et al., Prevalence and clinical implications of sarcopenic obesity in patients with solid tumours of the respiratory and gastrointestinal tracts: a population-based study, The Lancet Oncology 9 (2008) 629–635.

[25] K. Fearon, F. Strasser, S.D. Anker, I. Bosaeus, E. Bruera, R.L. Fainsinger, et al., Definition and classification of cancer cachexia: an international consensus, Lancet Oncol. 12 (2011) 489–495.

[26] J.P. Hakenjos, R. Richter, E.M. Dohmann, A. Katsiarimpa, E. Isono, C. Schwechheimer, MLN4924 is an efficient inhibitor of NEDD8 conjugation in plants, Plant Physiol. 156 (2011) 527–536.

[27] D. Yaffe, O. Saxel, Serial passaging and differentiation of myogenic cells isolated from dystrophic mouse muscle, Nature 270 (1977) 725–727.

[28] J.A. DeQuach, V. Mezzano, A. Miglani, S. Lange, G.M. Keller, F. Sheikh, et al., Simple and high yielding method for preparing tissue specific extracellular matrix coatings for cell culture, PLoS One 5 (2010) e13039.

[29] J.C. Hildyard, D.J. Wells, Identification and validation of quantitative PCR reference genes suitable for normalizing expression in normal and dystrophic cell culture models of myogenesis, PLoS Curr. 6 (2014) http://dx.doi.org/10.1371/currents.md.faafdde4bea8df4aa7d06cd5553119a6.

[30] T.J. Hinterberger, K.F. Barald, Fusion between myoblasts and adult muscle fibers promotes remodeling of fibers into myotubes *in vitro*, Development 109 (1990) 139–147.

[31] L. Silberstein, S.G. Webster, M. Travis, H.M. Blau, Developmental progression of myosin gene expression in cultured muscle cells, Cell 46 (1986) 1075–1081.

[32] M.A. Smith, Y.M. Yao, N.E. Reist, C. Magill, B.G. Wallace, U.J. McMahan, Identification of agrin in electric organ extracts and localization of agrin-like molecules in muscle and central nervous system, J. Exp. Biol. 132 (1987) 223–230.

[33] M.A. Milhollen, M.P. Thomas, U. Narayanan, T. Traore, J. Riceberg, B.S. Amidon, et al., Treatment-emergent mutations in NAEbeta confer resistance to the NEDD8-activating enzyme inhibitor MLN4924, Cancer Cell 21 (2012) 388–401.

[34] R.T. Swords, H.P. Erba, D.J. DeAngelo, D.L. Bixby, J.K. Altman, M. Maris, et al., Pevonedistat (MLN4924), a first-in-class NEDD8-activating enzyme inhibitor, in patients with acute myeloid leukaemia and myelodysplastic syndromes: a phase 1 study, Br. J. Haematol. 169 (2015) 534–543.

[35] M. Wang, B.C. Medeiros, H.P. Erba, D.J. DeAngelo, F.J. Giles, R.T. Swords, Targeting protein neddylation: a novel therapeutic strategy for the treatment of cancer, Expert Opin. Ther. Targets 15 (2011) 253–264.

[36] Y. Oikawa, R. Omori, T. Nishii, Y. Ishida, M. Kawaichi, E. Matsuda, The methyl-CpG-binding protein CIBZ suppresses myogenic differentiation by directly inhibiting myogenin expression, Cell Res. 21 (2011) 1578–1590.

[37] R. Geyer, S. Wee, S. Anderson, J. Yates, D.A. Wolf, BTB/POZ domain proteins are putative substrate adaptors for cullin 3 ubiquitin ligases, Mol. Cell 12 (2003) 783–790.

[38] L. Xu, Y. Wei, J. Reboul, P. Vaglio, T.H. Shin, M. Vidal, et al., BTB proteins are substrate-specific adaptors in an SCF-like modular ubiquitin ligase containing CUL-3, Nature 425 (2003) 316–321.

[39] L. Sun, J.S. Trausch-Azar, A. Ciechanover, A.L. Schwartz, Ubiquitin-proteasome-mediated degradation, intracellular localization, and protein synthesis of MyoD and Id1 during muscle differentiation, J. Biol. Chem. 280 (2005) 26,448–26,456.

[40] T. Wallach, K. Schellenberg, B. Maier, R.K. Kalathur, P. Porras, E.E. Wanker, et al., Dynamic circadian protein-protein interaction networks predict temporal organization of cellular functions, PLoS Genet. 9 (2013) e1003398.

[41] H. Suzuki, T. Chiba, M. Kobayashi, M. Takeuchi, T. Suzuki, A. Ichiyama, et al., IkappaBalpha ubiquitination is catalyzed by an SCF-like complex containing Skp1, cullin-1, and two F-box/WD40-repeat proteins, betaTrCP1 and betaTrCP2, Biochem. Biophys. Res. Commun. 256 (1999) 127–132.

[42] Y. Oikawa, E. Matsuda, T. Nishii, Y. Ishida, M. Kawaichi, Down-regulation of CIBZ, a novel substrate of caspase-3, induces apoptosis, J. Biol. Chem. 283 (2008) 14,242–14,247.

[43] S. Azmi, A. Ozog, R. Taneja, Sharp-1/DEC2 inhibits skeletal muscle differentiation through repression of myogenic transcription factors, J. Biol. Chem. 279 (2004) 52,643–52,652.

[44] P.S. Zammit, T.A. Partridge, Z. Yablonka-Reuveni, The skeletal muscle satellite cell: the stem cell that came in from the cold, J. Histochem. Cytochem. 54 (2006) 1177–1191.

[45] Z. Yablonka-Reuveni, The skeletal muscle satellite cell: still young and fascinating at 50, J. Histochem. Cytochem. 59 (2011) 1041–1059.

[46] D. Deponti, S. Francois, S. Baesso, C. Sciorati, A. Innocenzi, V. Broccoli, et al., Necdin mediates skeletal muscle regeneration by promoting myoblast survival and differentiation, J. Cell Biol. 179 (2007) 305–319.

[47] K.J. Wilson, H. Qadota, P.E. Mains, G.M. Benian, UNC-89 (obscurin) binds to MEL-26, a BTB-domain protein, and affects the function of MEI-1 (katanin) in striated muscle of *Caenorhabditis elegans*, Mol. Biol. Cell 23 (2012) 2623–2634.

[48] S. Lange, S. Perera, P. Teh, J. Chen, Obscurin and KCTD6 regulate cullin-dependent small ankyrin-1 (sAnk1.5) protein turnover, Mol. Biol. Cell 23 (2012) 2490–2504.

[49] F.B. Berry, Y. Miura, K. Mihara, P. Kaspar, N. Sakata, T. Hashimoto-Tamaoki, et al., Positive and negative regulation of myogenic differentiation of C2C12 cells by isoforms of the multiple homeodomain zinc finger transcription factor ATBF1, J. Biol. Chem. 276 (2001) 25,057–25,065.

[50] H. Qiu, N. Liu, L. Luo, J. Zhong, Z. Tang, K. Kang, et al., MicroRNA-17-92 regulates myoblast proliferation and differentiation by targeting the ENH1/Id1 signaling axis, Cell Death Differ. 23 (2016) 1658–1669.

[51] K. Langlands, X. Yin, G. Anand, E.V. Prochownik, Differential interactions of id proteins with basic-helix-loop-helix transcription factors, J. Biol. Chem. 272 (1997) 19,785–19,793.

[52] H. Faralli, E. Martin, N. Core, Q.C. Liu, P. Filippi, F.J. Dilworth, et al., Teashirt-3, a novel regulator of muscle differentiation, associates with BRG1-associated factor 57 (BAF57) to inhibit myogenin gene expression, J. Biol. Chem. 286 (2011) 23,498–23,510.

[53] M.F. Buas, S. Kabak, T. Kadesch, The notch effector Hey1 associates with myogenic target genes to repress myogenesis, J. Biol. Chem. 285 (2010) 1249–1258.

[54] J. Brocher, B. Vogel, R. Hock, HMGA1 down-regulation is crucial for chromatin composition and a gene expression profile permitting myogenic differentiation, BMC Cell Biol. 11 (2010) 64.

[55] M. Sekimata, Y. Homma, Regulation of Rb gene expression by an MBD2-interacting zinc finger protein MIZF during myogenic differentiation, Biochem. Biophys. Res. Commun. 325 (2004) 653–659.

[56] A. Ravel-Chapuis, T.E. Crawford, M.L. Blais-Crepeau, G. Belanger, C.T. Richer, B.J. Jasmin, The RNA-binding protein Staufen1 impairs myogenic differentiation via a c-myc-dependent mechanism, Mol. Biol. Cell 25 (2014) 3765–3778.

[57] K. Yuasa, N. Aoki, T. Hijikata, JAZF1 promotes proliferation of C2C12 cells, but retards their myogenic differentiation through transcriptional repression of MEF2C and MRF4 implications for the role of Jazf1 variants in oncogenesis and type 2 diabetes, Exp. Cell Res. 336 (2015) 287–297.

[58] X. Shi, A.M. Wallis, R.D. Gerard, K.A. Voelker, R.W. Grange, R.A. DePinho, et al., Foxk1 promotes cell proliferation and represses myogenic differentiation by regulating Foxo4 and Mef2, J. Cell Sci. 125 (2012) 5329–5337.

[59] G. Smaldone, L. Pirone, N. Balasco, S. Di Gaetano, E.M. Pedone, L. Vitagliano, Cullin 3 recognition is not a universal property among KCTD proteins, PLoS One 10 (2015) e0126808.

[60] A.X. Ji, A. Chu, T.K. Nielsen, S. Benlekbir, J.L. Rubinstein, G.G. Prive, Structural insights into KCTD protein assembly and Cullin3 recognition, J. Mol. Biol. 428 (2016) 92–107.

[61] E. Okochi-Takada, K. Nakazawa, M. Wakabayashi, A. Mori, S. Ichimura, T. Yasugi, et al., Silencing of the UCHL1 gene in human colorectal and ovarian cancers, Int. J. Cancer 119 (2006) 1338–1344.

[62] F. Gonnet, B. Bouazza, G.A. Millot, S. Ziaei, L. Garcia, G.S. Butler-Browne, et al., Proteome analysis of differentiating human myoblasts by dialysis-assisted two-dimensional gel electrophoresis (DAGE), Proteomics 8 (2008) 264–278.

[63] A.V. Gomes, D.S. Waddell, R. Siu, M. Stein, S. Dewey, J.D. Furlow, et al., Upregulation of proteasome activity in muscle RING finger 1-null mice following denervation, FASEB J. 26 (2012) 2986–2999.

[64] R.A. Powis, C.A. Mutsaers, T.M. Wishart, G. Hunter, B. Wirth, T.H. Gillingwater, Increased levels of UCHL1 are a compensatory response to disrupted ubiquitin homeostasis in spinal muscular atrophy and do not represent a viable therapeutic target, Neuropathol. Appl. Neurobiol. 40 (2014) 873–887.

[65] F. Chen, Y. Sugiura, K.G. Myers, Y. Liu, W. Lin, Ubiquitin carboxyl-terminal hydrolase L1 is required for maintaining the structure and function of the neuromuscular junction, Proc. Natl. Acad. Sci. U. S. A. 107 (2010) 1636–1641.

[66] S.M. Abmayr, G.K. Pavlath, Myoblast fusion: lessons from flies and mice, Development 139 (2012) 641–656.

[67] K. Rochlin, S. Yu, S. Roy, M.K. Baylies, Myoblast fusion: when it takes more to make one, Dev. Biol. 341 (2010) 66–83.

[68] V. Andres, K. Walsh, Myogenin expression, cell cycle withdrawal, and phenotypic differentiation are temporally separable events that precede cell fusion upon myogenesis, J. Cell Biol. 132 (1996) 657–666.

[69] D.P. Millay, J.R. O'Rourke, L.B. Sutherland, S. Bezprozvannaya, J.M. Shelton, R. Bassel-Duby, et al., Myomaker is a membrane activator of myoblast fusion and muscle formation, Nature 499 (2013) 301–305.

[70] L.A. Tintignac, H.R. Brenner, M.A. Ruegg, Mechanisms regulating neuromuscular junction development and function and causes of muscle wasting, Physiol. Rev. 95 (2015) 809–852.

[71] A. Burgess, S. Vigneron, E. Brioudes, J.C. Labbe, T. Lorca, A. Castro, Loss of human Greatwall results in G2 arrest and multiple mitotic defects due to deregulation of the cyclin B-Cdc2/PP2A balance, Proc. Natl. Acad. Sci. U. S. A. 107 (2010) 12,564–12,569.

[72] E.W. Godfrey, R.M. Nitkin, B.G. Wallace, L.L. Rubin, U.J. McMahan, Components of torpedo electric organ and muscle that cause aggregation of acetylcholine receptors on cultured muscle cells, J. Cell Biol. 99 (1984) 615–627.

[73] S. Nam, K. Min, H. Hwang, H.O. Lee, J.H. Lee, J. Yoon, et al., Control of rapsyn stability by the CUL-3-containing E3 ligase complex, J. Biol. Chem. 284 (2009) 8195–8206.

[74] Y. Chen, F.C. Ip, L. Shi, Z. Zhang, H. Tang, Y.P. Ng, et al., Coronin 6 regulates acetylcholine receptor clustering through modulating receptor anchorage to actin cytoskeleton, J. Neurosci. 34 (2014) 2413–2421.

[75] S. Luiskandl, B. Woller, M. Schlauf, J.A. Schmid, R. Herbst, Endosomal trafficking of the receptor tyrosine kinase MuSK proceeds via clathrin-dependent pathways, Arf6 and actin, FEBS J. 280 (2013) 3281–3297.

[76] R. Madhavan, Z.L. Gong, J.J. Ma, A.W. Chan, H.B. Peng, The function of cortactin in the clustering of acetylcholine receptors at the vertebrate neuromuscular junction, PLoS One 4 (2009) e8478.

[77] Z. Dai, X. Luo, H. Xie, H.B. Peng, The actin-driven movement and formation of acetylcholine receptor clusters, J. Cell Biol. 150 (2000) 1321–1334.

[78] J.A. Connolly, Role of the cytoskeleton in the formation, stabilization, and removal of acetylcholine receptor clusters in cultured muscle cells, J. Cell Biol. 99 (1984) 148–154.

[79] Z.W. Hall, B.W. Lubit, J.H. Schwartz, Cytoplasmic actin in postsynaptic structures at the neuromuscular junction, J. Cell Biol. 90 (1981) 789–792.

[80] A. Thirunavukarasou, G. Govindarajalu, P. Singh, V. Bandi, K. Muthu, S. Baluchamy, Cullin 4A and 4B ubiquitin ligases interact with gamma-tubulin and induce its polyubiquitination, Mol. Cell. Biochem. 401 (2015) 219–228.

[81] J. Yan, F. Yan, Z. Li, B. Sinnott, K.M. Cappell, Y. Yu, et al., The 3M complex maintains microtubule and genome integrity, Mol. Cell 54 (2014) 791–804.

[82] N.G. Starostina, J.M. Simpliciano, M.A. McGuirk, E.T. Kipreos, CRL2(LRR-1) targets a CDK inhibitor for cell cycle control in *C. elegans* and actin-based motility regulation in human cells, Dev. Cell 19 (2010) 753–764.

[83] A.M. Hudson, L. Cooley, Drosophila Kelch functions with cullin-3 to organize the ring canal actin cytoskeleton, J. Cell Biol. 188 (2010) 29–37.

[84] Y. Chen, Z. Yang, M. Meng, Y. Zhao, N. Dong, H. Yan, et al., Cullin mediates degradation of RhoA through evolutionarily conserved BTB adaptors to control actin cytoskeleton structure and cell movement, Mol. Cell 35 (2009) 841–855.

[85] J.R. Skaar, J.K. Pagan, M. Pagano, SCF ubiquitin ligase-targeted therapies, Nat. Rev. Drug Discov. 13 (2014) 889–903.

[86] N. Zheng, Q. Zhou, Z. Wang, W. Wei, Recent advances in SCF ubiquitin ligase complex: clinical implications, Biochim. Biophys. Acta 2016 (1866) 12–22.

[87] I.R. Watson, M.S. Irwin, M. Ohh, NEDD8 pathways in cancer, sine quibus non, Cancer Cell 19 (2011) 168–176.

[88] A.A. Domenighetti, P.H. Chu, T. Wu, F. Sheikh, D.S. Gokhin, L.T. Guo, et al., Loss of FHL1 induces an age-dependent skeletal muscle myopathy associated with myofibrillar and intermyofibrillar disorganization in mice, Hum. Mol. Genet. 23 (2014) 209–225.

[89] L.R. Smith, H.G. Chambers, R.L. Lieber, Reduced satellite cell population may lead to contractures in children with cerebral palsy, Dev. Med. Child Neurol. 55 (2013) 264–270.

[90] S. Lange, K. Gehmlich, A.S. Lun, J. Blondelle, C. Hooper, N.D. Dalton, et al., MLP and CARP are linked to chronic PKCalpha signalling in dilated cardiomyopathy, Nat. Commun. 7 (2016) 12,120.

[91] W.S. Rasband, ImageJ, U S National Institutes of Health, Bethesda, Maryland, USA, 1997–2016 (http://imagejnihgov/ij/).